



جمهورية العراق
وزارة التعليم العالي
والبحث العلمي
جامعة بابل

دراسة في السلوك الحراري للمساند
ذات التحميل العالي
رسالة

مقدمة إلى كلية الهندسة في جامعة بابل
كجزء من متطلبات نيل درجة ماجستير علوم
في الهندسة الميكانيكية
(ميكانيك تطبيقي)

أعدت من قبل

باسم رحيم صادق

بكالوريوس هندسة ميكانيكية

بِسْمِ اللّٰهِ الرَّحْمٰنِ الرَّحِیْمِ

اَقْرَأْ بِاسْمِ رَبِّكَ الَّذِي خَلَقَ (۱) خَلَقَ

الْاِنْسَانَ مِنْ عَلَقٍ (۲) اَقْرَأْ وَرَبُّكَ الْاَكْرَمُ

(۳) الَّذِي عَلَّمَ بِالْقَلَمِ (۴) عَلَّمَ الْاِنْسَانَ مَا لَمْ

يَعْلَمُ (۵)

صَدَقَ اللّٰهُ الْعَلِیُّ الْعَظِیْمُ

سورة العلق (الایات ۱-۵)

Republic of Iraq

Ministry of Higher Education

and Scientific Research

University of Babylon



**AN INVESTIGATION INTO THERMAL BEHAVIOR
OF HIGHLY LOADED BEARINGS**

A Thesis

Submitted to the College of Engineering

*University of Babylon in Partial Fulfillment of
Requirements for the Degree of Master of Science in
Mechanical Engineering*

(Applied Mechanics)

By Basim Raheim Sadiq

(B.Sc. 1981)

(November, 2006)

2006 A.M

1427 A.H

DEDICATION

To my supervisors

To my family

To my friends

SUPERVISOR CERTIFICATE

We certify that this thesis entitled "An Investigation Into Thermal Behavior of Highly Loaded Bearings " was prepared under our supervision at the Mechanical Engineering Department, University Of Babylon, Babylon – Iraq, as a partial fulfillment of the requirements for the degree of Master of Science in Mechanical Engineering.

Signature

Signature

Lecturer

Asst. Prof.

Dr. Basim A. Abass

Dr. Alaa' M. Hussein

Al-Maksosi

Al-Jesany

(Supervisor)

(Supervisor)

Date / /

Date / /

ACKNOWLEDGMENT

(In The Name of Allah, The Gracious, The Merciful)

First, of all I thank Allah who helped me in carrying out this work.

I wish to express my deep gratitude to my supervisors Dr. Basim A. Abass and Dr. Alaa' M. Hussein for their invaluable help, advice and encouragement during the various stages of the present work.

Finally, I record sincere gratitude to all those who have helped me throughout this research even by one word.

Basim

٢٠٠٦

ABSTRACT

Hydrodynamically lubricated journal bearings are considered to be a vital component of most of the rotating machines. It is used to support radial loads under wide range of speeds. In the journal bearing, pressure or hydrodynamic lift is generated in a thin lubricant oil film that separates the shaft and the bush, thus preventing metal to metal contact.

The steady state thermal behavior of hydrodynamic bearing is one of the most important subjects to be considered in designing this type of bearings for rotating machineries. For heavy machines, like cement mills, the maximum allowable bearing surface temperature is a major restriction of the running time for these machines.

In order to investigate the effect of lubricant viscosity on the performance of the journal bearing, a complete thermohydrodynamic analysis (THD) of a plain cylindrical journal system has been developed. The classical form of the Reynold's equation coupled with the energy equation and the heat conduction equation through the solids are solved numerically using a finite difference technique with appropriate boundary conditions. A full hydrodynamic journal bearing has been investigated and the obtained results have been checked by comparing it with another theoretical and experimental results of different workers. The computer's program, which was written in (FORTRAN – 90), was prepared to solve the above problem. Then it was used to investigate the performance of the partial arc journal bearing as that was used in a cement mills.

This investigation reveals that the oil viscosity has a pronounced influence on the bearing performance, and the effect of the temperature of the hollow shaft on the thermal behavior of the partial journal bearing in cement mill is the dominant operation parameter. The increase of the shaft temperature reduces the minimum oil film thickness which is limited the operation temperature of the journal bearing and running time of the cement mill can be increased by reducing the shaft temperature.

LIST OF CONTENTS

Acknowledgment	I
Abstract	II
List of contents	IV
Nomenclature	VII
<i>Chapter One – Introduction</i>	1
1.1 General	1
1.2 The Objectives of the Present Work	2
<i>Chapter Two – Literatures Review</i>	4
2.1 Introduction.....	4
2.2 Literatures review	5
<i>Chapter Three – Mathematical Model and Theory</i>	13
3.1 Coordinates system	13
3.2 Reynold's equation	14
3.3 Energy equation	16
3.4 Heat conduction equation	16
3.5 Equation of state.....	17
3.6 Attitude angle.....	17

- 3.7 Boundary conditions..... 18
- 3.8 Numerical analysis..... 19
 - 3.8.1 Mesh generation 19
 - 3.8.2 Reynold's equation..... 21
 - 3.8.3 Energy equation 23
 - 3.8.4 Heat conduction equation 24
 - 3.8.5 Solution procedure 25
 - 3.8.6 Solution procedure for partial journal bearing 28
- 3.9 Computer program 29

Chapter Four –Result and discussion 36

- 4.1 verification of the computer program 36
- 4.2 Thermohydrodynamic analysis of full journal bearing..... 37
- 4.3 Thermohydrodynamic analysis of partial journal bearing... 39

Chapter Five – Conclusions and Suggestions for Future work. 63

- 5.1 Conclusions 63
- 5.2 Suggestions for Future Work 64

References 66

Appendices 69

Appendix A Derivation of the Reynold's Equation 69

Appendix B Derivation of the Energy 72

NOMENCLATURE

The following symbols are generally used throughout the text.

Others are defined as when used.

SYMBOL	DESCRIPTION	UNITS
c	Radial clearance	m
C_o	Specific heat of lubricant	J/kg. °C
D	Diameter of journal	m
e	Journal eccentricity	m
h	Oil film thickness	m
h_{conv}	Convective heat transfer coefficient	w/m ² . °C
h_{max}	Maximum oil film thickness	m
h_{min}	Minimum oil film thickness	m
\bar{h}	dimensionless oil film thickness (h/c)	
i, j, k	The indexes increases along x, y, z axes	
k_b	Thermal conductivity of the bush	w/m. °C
k_{oil}	Thermal conductivity of lubricant	w/m. °C
k_s	Thermal conductivity of the shaft	w/m. °C
k_o, k_1, k_2	Oil viscosity coefficient	

N	Journal speed	r.p.m
L	Bearing length	m
P	Oil Pressure	N/m ²
p_{atm}	Atmosphere pressure	N/m ²
p_s	Oil supply pressure	N/m ²
\bar{p}	Dimensionless oil Pressure = $(p/\eta_{in})(\frac{R}{U})(\frac{c}{R})^2$	
\bar{p}_s	Dimensionless oil supply Pressure = $(p_s/\eta_{in})(\frac{R}{U})(\frac{c}{R})^2$	
Q_{rec}	Recirculation oil flow rate	m ³ /s
Q_l	Axial leakage oil flow rate	m ³ /s
Q_{in}	Supply oil flow rate	m ³ /s
R	Journal radius	m
r_b	Bush radius	m
r_{bin}	Bush inner radius	m
r_{bout}	Bush outer radius	m
t	Oil temperature	°C
ta	Ambient temperature	°C
t _b	Bush temperature	°C
t _{bo}	Bush outer surface temperature	°C

t_{in}	Inlet oil temperature	$^{\circ}C$
t_r	Recirculating oil temperature	$^{\circ}C$
t_s	Shaft temperature	$^{\circ}C$
t_{si}	Inner temperature of the hallow shaft	$^{\circ}C$
\bar{t}	Dimensionless temperature = t / t_{in}	
U	Shaft speed	m/s
u	Fluid velocity component in x direction	m/s
\bar{u}	Dimensionless velocity = u/U	
v	Fluid velocity component in y direction	m/s
\bar{v}	Dimensionless velocity = $v/U(R/c)$	
w	Fluid velocity component in z direction	m/s
\bar{w}	Dimensionless velocity = w/U	
W	Bearing load capacity	N
x,y,z	Coordinate system	
$\bar{\bar{x}}, \bar{\bar{y}}, \bar{\bar{z}}$	Dimensionless coordinate system $\bar{\bar{x}} = \frac{x}{R}, \quad \bar{\bar{y}} = \frac{y}{h}, \quad \bar{\bar{z}} = \frac{z}{L}$	

Greek symbols

Symbol	Description	Units
ε	Eccentricity Ratio	-
$\varepsilon_{\bar{p}}, \varepsilon_{\bar{t}}$	Errors Ratios	-
μ	Lubrication viscosity	pa . s
μ_{in}	Inlet lubrication viscosity	pa . s
$\frac{\mu}{\mu_{in}}$	Dimensionless viscosity = $\frac{\mu}{\mu_{in}}$	
ρ	Density of oil	kg/m ³
τ	Shear Stress	N/m ²
ϕ	Bearing Attitude Angle	rad
ω	Journal Rotational Speed	rad/s

Superscript

—	Dimensionless quantity
---	------------------------

الخلاصة

تعتبر المساند الزيتية من الأجزاء الرئيسية في معظم المعدات الثقيلة الدوارة في الصناعة. في هذه المساند الضغط المتولد في طبقة خفيفة من الزيت يقوم برفع المحور الدوار ومنع تماسه مع الأجزاء الثابتة. لغرض دراسة السلوك الحراري للمساند الزيتية وتأثير عوامل التشغيل المختلفة على هذا السلوك لكونه من أهم العوامل المحددة في تصميم المساند الزيتية للمكائن الدوارة. وفي بعض التطبيقات كما في طواحين الاسمنت تكون حرارة جسم المسند أساس تحديد ساعات التشغيل. تم اعتماد نظرية الثرموهيدرودينامك لغرض إجراء هذه الدراسة و تضمنت المعالجة النظرية للموضوع حل المعادلات الحاكمة عددياً وهي معادلة رينولدز التي تحكم ضغط طبقة الزيت ومعادلة الطاقة التي تحكم انتقال الحرارة في طبقة الزيت ومعادلة انتقال الحرارة في الأجسام الصلبة إضافة إلى الشروط الحدية. تم إعداد برنامج مكتوب بلغة الفورتران (٩٠) لحل المعادلات الحاكمة أعلاه أنياً. بعد ذلك تم تقييم للنتائج بمقارنتها بنتائج بحوث سابقه منشوره ومن مصادر معتبرة أظهرت هذه المقارنات قرب نتائج البحث في احتساب السلوك الحراري من النتائج الواقعية. بعد هذه الخطوه تم احتساب تأثير مختلف العوامل التشغيلية على التوزيع الحراري والضغط داخل طبقة الزيت وحرارة جسم المسند وفي المستوى الوسطي. كذلك تضمنت الدراسة دراسة السلوك الحراري للمساند الجزئية المستخدمة في طواحين الاسمنت والتي يصل تحميلها إلى أكثر من (٤٥٠)طن مع وجود حرارة منتقلة عبر الشفت المجوف للمسند. تبين من خلال الدراسة التأثير الأساسي لحرارة الشفت المجوف على ارتفاع حرارة جسم المسند وبالتالي التسبب في توقف الماكنة لذا يتطلب إدامة التشغيل معالجة الارتفاع في حرارة الشفت لكونه المحدد الأساسي لساعات التشغيل وحسب الدراسة.

APPENDIX-A

Reynold's equation deriving

The Renold's equation is derived with the following general assumptions:

- 1- Laminar flow.
- 2- Incompressible fluid.
- 3- Pressure gradient across the film is negligible.
- 4- $h/l \ll 1$
- 5- body force and inertia forces are negligible.
- 6- Steady state flow.
- 7- The lubricant is Newtonian.

The starting point is the condition of equilibrium of small element in the oil film with sides length (dx, dy, dz) under the action of the viscose shear stresses and oil pressure as follow:

$$\Sigma F_x = 0$$

$$\frac{\partial \tau_{yx}}{\partial y} = \frac{\partial p}{\partial x} \quad \dots\dots(A-1)$$

$$\Sigma F_z = 0$$

$$\frac{\partial \tau_{yz}}{\partial y} = \frac{\partial p}{\partial z} \quad \dots\dots(A-2)$$

And from assumption 3:

$$\frac{\partial p}{\partial y} = 0$$

From the Newton's law of viscous flow:

$$\tau_{yx} = \mu \frac{\partial u}{\partial y} \quad \dots\dots(A-3)$$

$$\tau_{yz} = \mu \frac{\partial w}{\partial y} \quad \dots\dots(A-4)$$

Where τ the fluid shear stress.

Combine equations (A-1), (A-3), and equations (A-2), (A-4) to get:

$$\frac{\partial}{\partial y} \left(\mu \frac{\partial u}{\partial y} \right) = \frac{\partial p}{\partial x} \quad \dots\dots(A-5)$$

$$\frac{\partial}{\partial y} \left(\mu \frac{\partial w}{\partial y} \right) = \frac{\partial p}{\partial z} \quad \dots\dots(A-6)$$

Integrating equations (A-5), (A-6) twice to get the fluid velocity components (u, w) in (x, z) directions, and for first component as below:

Where viscosity (μ) is a variable quantity.

$$\mu \frac{\partial u}{\partial y} = \frac{\partial p}{\partial x} y + c_1 \quad \dots\dots(A-7)$$

Then:

$$\frac{\partial u}{\partial y} = \frac{1}{\mu} \frac{\partial p}{\partial x} y + \frac{c_1}{\mu} \quad \text{.....(A-8)}$$

$$u = \frac{\partial p}{\partial x} \int_0^y \frac{y}{\mu} dy + c_1 \int_0^y \frac{1}{\mu} dy + c_2 \quad \text{.....(A-9)}$$

Where c_1, c_2 are constants can be found from the following boundary conditions:

$$u = 0 \quad \text{at} \quad y = 0$$

And

$$u = U \quad \text{at} \quad y = h \quad \text{.....(A-10)}$$

Substitute equation (A-10) in equation (A-9), the value of constants c_1, c_2 can be evaluated as:

$$c_2 = 0$$

$$c_1 = (U - \frac{\partial p}{\partial x} \int_0^h \frac{y}{\mu} dy) / \int_0^h \frac{1}{\mu} dy \quad \text{.....(A-11)}$$

Substitute equation (A-11) in equation (A-9) to obtain the velocity component in x direction as below:

$$u = \frac{\partial p}{\partial x} \left(-\frac{\int_0^h \frac{y}{\mu} dy \int_0^y \frac{1}{\mu} dy}{\int_0^h \frac{1}{\mu} dy} + \int_0^y \frac{1}{\mu} dy \right) + U \frac{\int_0^y \frac{1}{\mu} dy}{\int_0^h \frac{1}{\mu} dy} \quad \text{.....(A-12)}$$

By the same procedure and the following boundary conditions:

$$w = 0 \quad \text{at} \quad y = 0$$

And

$$w = 0 \quad \text{at} \quad y = h \quad \text{.....(A-13)}$$

The velocity component (w) in z direction as below:

$$w = \frac{\partial p}{\partial z} \left(\int_0^y \frac{y}{\mu} dy - \frac{\int_0^h \frac{y}{\mu} dy \int_0^y \frac{1}{\mu} dy}{\int_0^h \frac{1}{\mu} dy} \right) \quad \text{.....(A-14)}$$

For a column (h) fixed in space, (m_x, m_z) the mass flows per unit width in the (x, z) directions and for the condition of continuity of mass:

$$\frac{\partial m_x}{\partial x} + \frac{\partial m_z}{\partial z} = 0 \quad \text{.....(A-15)}$$

Where:

$$m_x = \rho \int_0^h u dy \quad \text{.....(A-16)}$$

Substitute equation (A-13) in equation (A-16) to obtain:

$$m_x = \rho \int_0^h \left(\frac{\partial p}{\partial x} \left(- \frac{\int_0^y \frac{y}{\mu} dy \int_0^y \frac{1}{\mu} dy}{\int_0^h \frac{1}{\mu} dy} + \int_0^y \frac{1}{\mu} dy \right) + U \frac{\int_0^y \frac{1}{\mu} dy}{\int_0^h \frac{1}{\mu} dy} \right) dy \quad \text{.....(A-17)}$$

And

$$m_z = \rho \int_0^h w dy \quad \text{.....(A-18)}$$

Substitute equation (A-14) in equation (A-18) to obtain:

$$m_z = \rho \int_0^h \left(\frac{\partial p}{\partial z} \left(\int_0^y \frac{y}{\mu} dy - \frac{\int_0^h \frac{y}{\mu} dy \int_0^y \frac{1}{\mu} dy}{\int_0^h \frac{1}{\mu} dy} \right) \right) dy \quad \dots\dots(A-19)$$

Substitute equations (A-17), (A-19) in equation (A-16) to obtain:

$$\frac{\partial}{\partial x} \left(\rho \int_0^h \left(\frac{\partial p}{\partial x} \left(- \frac{\int_0^h \frac{y}{\mu} dy \int_0^y \frac{1}{\mu} dy}{\int_0^h \frac{1}{\mu} dy} + \int_0^y \frac{1}{\mu} dy \right) + U \frac{\int_0^y \frac{1}{\mu} dy}{\int_0^h \frac{1}{\mu} dy} \right) dy \right) +$$

$$\frac{\partial}{\partial z} \left(\rho \int_0^h \left(\frac{\partial p}{\partial z} \left(\int_0^y \frac{y}{\mu} dy - \frac{\int_0^h \frac{y}{\mu} dy \int_0^y \frac{1}{\mu} dy}{\int_0^h \frac{1}{\mu} dy} \right) \right) dy \right) = \dots\dots(A-20)$$

Substitute the dimensionless form of parameters in equation (A-20), the dimensionless form of Reynold's equation:

$$\frac{\partial}{\partial \bar{x}} \left(\bar{F} \bar{h}^3 \frac{\partial \bar{P}}{\partial \bar{x}} \right) + \left(\frac{R}{L} \right)^2 \frac{\partial}{\partial \bar{z}} \left(\bar{F} \bar{h}^3 \frac{\partial \bar{P}}{\partial \bar{z}} \right) = \frac{\partial}{\partial \bar{x}} \left(\bar{G} \bar{h} \right) \quad \dots\dots(A-21)$$

Where:

$$\bar{F} = \frac{\int_0^1 \left(\int_0^1 \frac{\bar{y}}{\bar{\mu}} d\bar{y} \int_0^{\bar{y}} \frac{1}{\bar{\mu}} d\bar{y} - \int_0^1 \frac{\bar{y}}{\bar{\mu}} d\bar{z} \int_0^1 \frac{1}{\bar{\mu}} d\bar{y} \right) d\bar{y}}{\int_0^1 \frac{1}{\bar{\mu}} d\bar{y}} \quad \dots\dots(A-22)$$

$$\bar{G} = \frac{\int_0^1 \left(\int_0^{\bar{y}} \frac{1}{\bar{\mu}} d\bar{y} \right) d\bar{y}}{\int_0^1 \frac{1}{\bar{\mu}} d\bar{y}} \quad \dots\dots(A-23)$$

Appendix-B

Energy equation deriving

The energy equation for a lubricant film with the following assumption:

1- Heat conduction in the x and z directions have been ignored (small value).

2- The lubricant density and specific heat have been taken constant values.

It is given as :

$$\frac{\partial}{\partial x}(\rho C_o u t) + \frac{\partial}{\partial y}(\rho C_o v t) + \frac{\partial}{\partial z}(\rho C_o w t) = \frac{\partial}{\partial y} \left(k_{oil} \frac{\partial t}{\partial y} \right) + \mu \left[\left(\frac{\partial u}{\partial y} \right)^2 + \left(\frac{\partial w}{\partial y} \right)^2 \right] \quad \dots\dots(B-1)$$

Where the left side of the equation is the convection term, and the right side is the heat conduction across the lubricant film and the heat generated due to the viscose shear.

Then the equation (B-1) is solved as below:

$$\rho C_o t \left(\frac{\partial u}{\partial x} + \frac{\partial v}{\partial y} + \frac{\partial w}{\partial z} \right) + \rho C_o \left(u \frac{\partial t}{\partial x} + v \frac{\partial t}{\partial y} + w \frac{\partial t}{\partial z} \right) = \frac{\partial}{\partial y} \left(k_{oil} \frac{\partial t}{\partial y} \right) + \mu \left[\left(\frac{\partial u}{\partial y} \right)^2 + \left(\frac{\partial w}{\partial y} \right)^2 \right]. \quad (\text{B-}\Upsilon)$$

For continuity condition of lubricant flow:

$$\left(\frac{\partial u}{\partial x} + \frac{\partial v}{\partial y} + \frac{\partial w}{\partial z} \right) = 0 \quad \text{.....}(\text{B-}\Upsilon)$$

Then:

$$\rho C_o \left(u \frac{\partial t}{\partial x} + v \frac{\partial t}{\partial y} + w \frac{\partial t}{\partial z} \right) = \frac{\partial}{\partial y} \left(k_{oil} \frac{\partial t}{\partial y} \right) + \mu \left[\left(\frac{\partial u}{\partial y} \right)^2 + \left(\frac{\partial w}{\partial y} \right)^2 \right] \quad \text{.....}(\text{B-}\xi)$$

To transform energy equation to the dimensionless form, the coordinate transformation as follows:

$$\bar{x} = \frac{x}{R} : \text{coordinate in circumferential direction}$$

$$\bar{y} = \frac{y}{h} : \text{coordinate in the oil film thickness direction}$$

$$\bar{z} = \frac{z}{L} : \text{coordinate in the axial direction}$$

For the x coordinate:

$$\left. \frac{\partial t}{\partial x} \right|_{y \text{ constant}} = \left. \frac{\partial t}{\partial \bar{x}} \right|_{\bar{y} \text{ constant}} + \frac{\partial t}{\partial y} \frac{\partial \bar{y}}{\partial x} \quad \text{.....}(\text{B-}\omicron)$$

Where:

$$\frac{\partial \bar{y}}{\partial x} = \frac{\partial}{\partial x} \left(\frac{y}{h} \right) \quad \dots\dots(B-6)$$

Then:

$$\frac{\partial \bar{y}}{\partial x} = -\frac{y}{h^2} \frac{\partial h}{\partial x} \quad \dots\dots(B-7)$$

So:

$$\frac{\partial \bar{y}}{\partial x} = -\frac{\bar{y}}{h} \frac{\partial h}{\partial x} \quad \dots\dots(B-8)$$

Substitute equation (B-8) in equation (B-6):

$$\frac{\partial t}{\partial x} = \frac{\partial t}{\partial x} - \frac{\bar{y}}{h} \frac{\partial h}{\partial x} \frac{\partial t}{\partial \bar{y}} \quad \dots\dots(B-9)$$

For the z coordinate:

$$\left. \frac{\partial t}{\partial z} \right|_{y \text{ constant}} = \left. \frac{\partial t}{\partial z} \right|_{\bar{y} \text{ constant}} + \frac{\partial t}{\partial \bar{y}} \frac{\partial \bar{y}}{\partial z} \quad \dots\dots(B-10)$$

The lubricant film thickness (h) is assumed to be independent on z so:

$$\frac{\partial \bar{y}}{\partial z} = -\frac{y}{h^2} \frac{\partial h}{\partial z} = 0 \quad \dots\dots(B-11)$$

Substitute equation (B-11) in equation (B-10):

$$\left. \frac{\partial t}{\partial z} \right|_{y \text{ constant}} = \left. \frac{\partial t}{\partial z} \right|_{\bar{y} \text{ constant}} \quad \dots\dots(B-12)$$

Substitute the dimensionless form of parameters and the coordinates transformation equations (B-9), (B-12) in equation (B-4), the dimensionless form of the energy equation is:

$$\lambda_1 \bar{u} \frac{\partial \bar{t}}{\partial \bar{x}} + \lambda_1 \left(\frac{\bar{v}}{\bar{h}} - \bar{u} \frac{\bar{y}}{\bar{h}} \frac{\partial \bar{h}}{\partial \bar{x}} \right) \frac{\partial \bar{t}}{\partial \bar{y}} = \frac{1}{\bar{h}^2} \lambda_2 \frac{\partial^2 \bar{t}}{\partial \bar{y}^2} + \frac{\bar{\mu}}{\bar{h}^2} \lambda_3 \left[\left(\frac{\partial \bar{u}}{\partial \bar{y}} \right)^2 + \left(\frac{\partial \bar{w}}{\partial \bar{y}} \right)^2 \right] \quad \text{.....(B-13)}$$

Where:

$$\lambda_1 = \frac{\rho U C_o R}{k_{oil}} \quad \text{.....(B-14)}$$

$$\lambda_2 = \left(\frac{R}{c} \right)^2 \quad \text{.....(B-15)}$$

$$\lambda_3 = \left(\frac{R}{c} \right)^2 \frac{\mu_i U^2}{k_{oil} t_{in}} \quad \text{.....(B-16)}$$

INTRODUCTION



General

Hydrodynamic bearings are used in industry to support rotating shafts of heavy machines, they are considered as a good choice due to their constructive simplicity, reliability, efficiency, and low cost. The radial hydrodynamic bearings, with oil as a lubricant, are widely used. Oil temperature inside the bearing affected by the applied operation conditions, oil viscosity as known varies substantially with the temperature leading to decrease the bearing load capacity, consequently, thermal effect in hydrodynamic lubrication plays a crucial role in prediction of the bearing performance.

In the present work the bearing which support the cement mill in the cement plants has been investigated. This bearing represent the main part of the mill which is a cylindrical body with a diameter reaches sometimes to more than (2) meters and weight reaches to (1000)T. The mill body is supported by two partial journal bearings with cooled oil supplying system. It was shown during operation that the maximum allowable bearing surface temperature is the major restriction of the running time, especially during summer season. It is required that the bearings maximum surface temperature is usually to be well below (100)°C. Hence more than this limit a margin of safety is usually imposed. When the maximum temperature is reached the mill will be stopped until the bearing is cooled which is time consuming, it consumes about more than (10) hours, leading to lose the production in the critical time. Two sources of heat are available with this type of journal bearings, the heat dissipated due to the viscous effect and that produced due to the milling process. In order to save the running time of the mill, the temperature of bearing bush metal must be kept below the maximum allowable temperature. The effect of different operation parameters and geometric factors on the bearing behavior must be

studied. The present work consists of a theoretical analysis to predict the thermal behavior of a finite length full and partial journal bearings by using thermohydrodynamic theory. A full journal bearing with a single groove located at the crown of the bearing on the line parallel to the load direction and a partial arc bearing with a 120° were investigated. The governing equation namely, Reynold's equation coupled with the energy equation at the lubricant and the heat conduction equation in the bearing body and shaft were solved with appropriate boundary conditions by using a suitable finite differences method. Iterative scheme with successive under relaxation was employed to obtain the pressure and the temperature field in the oil film and the bearing body. For this purpose computer program was prepared and written using (FORTRAN 90) to solve the governing equations. The obtained results, for full journal bearing, are compared with theoretical and experimental results from available published works. The computer program was modified to investigate the performance of 120° partial arc journal bearing which is used in cement mills with hollow shaft rotating with low speed. The effect of the operating parameters, include the hollow shaft temperature, on the thermal behavior of the partial journal bearing are studied and deduced the main reason of the temperature rising, and the effective way to solve the problem can be decided.

Under the normal operating conditions, the lubricant undergoes a significant change in temperature along the circumferential direction, which causes a change in viscosity and other bearing performance parameters such as minimum film thickness, load carrying capacity, leakage flow rate, and power loss.

Hence the main objective of this work is to establish a complete thermohydrodynamic analysis for a full journal bearing via the following steps :-

- ١- The development of a mathematical model for a finite length journal bearing.
- ٢- The preparation of a computer program to solve the governing equations using a suitable numerical technique.
- ٣- Studying of the effect of different operating parameters on the performance of the bearing.

The other main objective of this work is to modify the computer program mentioned above to analyze the causes of the bearing failure which is used to support the cement mill in Karbala cement plant.

LITERATURES REVIEW

٢.١

Introduction

The study of the thermal effect on bearing performance has been considered to be an important subject since the evolution of tribology as a field of study. The driving force behind this, is the frequent failure of tribological component due to metal-to-metal contact and the associated rise in the frictional heating. Hence, for an accurate investigation to the behavior of the bearing, thermal effects in lubrication must be taken into account, the performance of hydrodynamic bearings is a strong function of lubricant viscosity, which is known to vary substantially with temperature. Different methods were proposed to take the effect of temperature rise on the

performance of journal bearing. Thermal effects are primarily limited to employ a specific value of the viscosity, called effective viscosity, according to the average temperature rise in the bearing. The most draw back of this method that it dose not provide any information about the peak temperature, which is one of the most important subject to be considered in bearing design. Adiabatic solution for the journal bearing was used including variable viscosity and a simple energy equation was solved uncoupled with Reynold's equation. In this case, it was assumed that the heat generated within the lubricant film is completely carried away by the oil and the heat losses from the oil film to the boundary surfaces have been ignored and the temperature at any point is taken to be constant across the oil film. This method can provide a rough value of maximum temperature. The incorporation of the variable viscosity is of the most importance, first because it affects all major performance items, secondly because it can provide the value of (T_{max}) which is one of the two basic mechanisms of the failure of hydrodynamic bearings, (h_{min}) is the other one. In the thermohydrodynamic (THD) analysis of the journal bearing, which considers the temperature and viscosity distribution through the oil film, is based on the solution of Reynold's equation coupled with the energy equation in the lubricant flow and the heat conduction equation in the bearing bush and the shaft, hence predicting bearing performance more accurately. The bearing temperature field requires proper assessment of heat conduction from the lubrication to the boundary surfaces, i.e the journal and the stationary housing, as well as the heat loss to the ambient by means of convection. The following are brief review to the literatures related to the field.



Literatures review

Pinkus and Bupara, [1], offered a method for the analysis of the finite journal bearing including variable oil viscosity with the assumption that the heat generated within the lubricant film is completely carried away by the fluid and hence the heat losses from the film to the boundary surfaces are ignored. The temperature at any point was taken to be constant across the oil film. The energy equation is decoupled from the Reynolds equation and it was solved, by neglecting the pressure gradient terms, to get the temperature within the film at any angular position. They got the performance parameters for three sizes of two axial- groove journal bearing such as load, maximum temperature, oil flow, etc.

Suganami and Szeri, [1], contrasted thermal performance of 10° degree partial arc short journal bearing with the results of the classical theories (isothermal, adiabatic) via a restricted parametric study. The problem was solved according to the following boundary conditions:

At the leading edge of the arc the temperature is the inlet oil temperature and at the trailing edge is zero normal gradient. At the oil film-bearing interface both the temperature and the heat flow are continuous. At low speeds the shaft surface is assumed to be at a uniform temperature while at high speeds is assumed to be insulated against heat flow.

Thermal effects are found to reduce load capacity in every case investigated and this reduction is small at small eccentricities and significant at large eccentricities .

Cowking, [2], described a technique to solve the Reynolds equation and energy equation for multi-arc journal bearing. The technique is based on the assumption that the temperature of the oil film is a function of the angular direction only. Theoretical results obtained for the maximum bearing temperature and they compared with that for two-arc test bearing. It was concluded that the bearing temperature over-estimates at low speeds and under-estimates at high speed.

Seireg and Dandage, [3], constructed a procedure to evaluate the performance of the journal bearing by using isoviscous theory with modified sommerfeld number which can replace the isoviscous sommerfeld number. The procedure was based on experimental thermohydrodynamic consideration. The empirical point that for any particular eccentricity, oil viscosity, and inlet temperature, there exists a speed where the isoviscous theory predicts the same magnitude of maximum pressure as that measured experimentally, but the variation of it with inlet temperature is different. This method is useful to provide the designer with an alternate method for selecting the main bearing parameters in critical application.

Ferron , et al. [4], studied the thermal effect in a finite journal bearing theoretically and experimentally. The thermohydrodynamic theory was used to predict the oil film pressure and the temperature through both the oil film and the solid housing. The Reynolds boundary condition had been adapted to solve the Reynolds equation while the temperature on the solid surfaces had been given by the heat flux continuity with constant shaft and inlet zone temperatures. They showed that the theoretical and experimental results obtained for oil film pressure are in good agreement, while

the measured maximum temperature is always higher than the theoretical value due to the uncertainties of the bush thermal conductivity as it was justified.

Mitsui , et al. [1], performed an experimental and theoretical analysis for the cooling effect of the oil supply in a circular journal bearing on the bases of (THD) analysis. The initial temperature distribution of the oil film just behind the oil inlet was calculated by using experimental mixing coefficient, which is defined as a participating ratio of the recirculation oil in the mixing process. A transparent plastic bearing was used to observe the film flow in the cavitated region .

The correlation between the supply oil flow rate and the mixing coefficient was conjecture. It was obtained that as the mixing coefficient increases the oil film temperature at respective depths in thickness tends to rise after the mixing process. Hence, the journal surface temperature is influenced thereby.

Lund and Hansen, [2], presented an analysis to solve the energy equation for the journal bearing oil film. The analysis approximates the oil temperature profile across the oil film thickness by a fourth order polynomial and ignored the variation of the viscosity across oil film thickness. The solution was used to estimate the temperature of the journal, bearing sleeve, and the oil film. The viscosity distribution obtained was used to solve the Reynolds' equation to obtain the pressure distribution in the oil film. Iteration is required between the energy and Reynolds equations because of the coupling through the pressure induced flow in the oil film.

The experimental part of the investigation shows that the calculated results, for two-axial groove journal bearing, compared with experimental measurements are satisfactory.

Mitsui, et al. [3], studied the effect of the journal speed, lubrication viscosity, and clearance ratio on the maximum bearing temperature and its location experimentally and compared it with the theoretical results published in [1]. They showed that the experimental result agrees with the theoretical one except in the region of the groove because of the reverse oil flow in the region. The maximum bearing temperature (T_{bmax}) increases with increasing journal speed and using more viscous lubricant. The maximum bearing temperature and the minimum oil film thickness locations moves with the journal direction as the journal speed increases. The surface temperature rise also increases with decreasing the radial clearance. The location of the maximum bearing temperature moves much than (h_{min}) do in reverse direction of the journal rotation.

The higher viscosity of the oil cause a higher temperature over the whole bearing surface due to the increased in shear rate.

Ferron et al. [9], conducted experimental and theoretical investigations based on a general thermohydrodynamic theory. During this work the effect of the thermal displacement of the shaft and the bush on the oil film thickness has been investigated. A good agreement between theoretical and experimental result is obtained when thermal deformations together with the differential thermal dilatation between the bearing and the shaft are considered.

Heshmat, and Pinkus, [10], offered a conceptual and an experimental investigation for the mixing mechanism of the cold and hot lubricant at inlet to the hydrodynamic bearing in terms of oil flow and temperatures. They constructed an equation to determine the mixing inlet temperature as a function of a range of operating conditions and bearing sizes correlated in terms of an appropriate mixing function .

Junichi, [11], conducted an extensive theoretical and an experimental investigation to determine the bearing metal and oil film temperature of circular journal bearings. The following conclusions were derived for the effects of the journal bearing speed, clearance ratio, lubricant viscosity, and load on the bearing temperature and were examined experimentally. The effects of the journal bearing clearance ratio, lubrication viscosity and loading on the bearing temperature has been investigated. This work led to an important conclusions such as that the maximum temperature increases considerably with the increase of journal speed, lubricant viscosity and with the decrease of clearance ratio.

The angular position of (T_{bmax}) varies considerably towards the direction of journal rotation from the upper stream side of the location of minimum film thickness to the lower stream side as the journal speed increases. The change of angular position of (T_{bmax}) is greater than that of (h_{min}) while the contrary happens with the decrease of clearance ratio. The value of (T_{bmax}) and the maximum oil film temperature dose not vary so much with the increase of load for any constant value of speed.

Khonsari and Estahanian, [12], extended the thermohydrodynamic theory to include the effect of solid particles carried by the oil in the hydrodynamically lubricated journal bearings. For a liquid-solid case, an experimental investigation indicated that if the solid particles are small, they will pass through the minimum film thickness and the shear stress relation can be classified as Newtonian fluid but the viscosity of the mixture (oil and solid) depends on the mixture ratio by weight, while if the particles size are larger than the minimum oil film thickness the relation will no longer be classified as Newtonian fluid. After the numerical solution, it was observed that the bearing temperatures are significantly increased by the existence of solid particles as compared to that of the clean oil case.

Khonsari and Kim, [13], conducted an extensive investigation to the seizure phenomenon occurs in the journal bearings during the start-up process when the shaft is in direct dry contact with the bush, due to the long time the bearing being unused or when the lubricant supply to the bearing is blocked, the paper predict how long time it was taken before seizure was set in. It is assumed that seizure occurs due to a complete loss in clearance resulting directly from thermal expansion of the shaft as it rubs internally against the bush surface.

Khonsari et al. [14], performed an extensive set of thermohydrodynamic simulation. They presented the results in the form of generalized design chart which enables one to predict the maximum temperature and the effective bearing temperatures.

Ma and Taylor, [15], conducted an experimental investigation on the thermal effects on the plain and elliptical journal bearings. Their investigation shows that the temperature variation is significant along the circumferential direction but not in the axial direction.

Fillon, et al. [16], experimented the effect of inlet oil groove location and supply pressure on the performance of single-axial groove journal bearing. The location of the inlet groove was changed in the test from (-30) to (+30) degrees in relation to the load line.

The experimental results showed that comparatively to the journal bearing with a groove on the load line, the location of the groove (-30) degrees has originated a reduction in the operating temperatures, oil flow rate and increase in the maximum hydrodynamic pressure. For location of (+30)degrees a reduction in operating temperatures, increase in the oil flow rate and increase in the

maximum hydrodynamic pressure. The increasing of the oil supply pressure increases the oil flow rate with a decrease in the bearing operating temperature and increases in maximum hydrodynamic pressure (for fixed applied load).

Pierre and Fillon, [17], analyzed the effects of various geometric factors and operating conditions on the journal bearing behaviour. They concluded that the operating temperature of the journal bearing is influenced by the rotational speed whatever the load values (other parameters are fixed), while at low speed, the minimum oil film thickness depends greatly on the applied load. For the high speed the effect of the speed becomes higher due to the increasing hydrodynamic effects. At low-load conditions, the rotational speed has nearly no influence on the maximum oil pressure, but at a high-load, the increase in speed reduces the maximum pressure. The use of thicker oil induces a higher operation temperature and not greatly affects the maximum pressure although a slight decrease occurs at a high load and low speeds due to the higher values of the minimum film thickness. Decreasing the bearing length leads to an increase in operation temperature and maximum pressure. Higher clearance leads to an increase in the axial flow rate particularly under high applied loads and high rotational speeds. The operation temperature decreases when the radial bearing clearance increases.

K. Hatakenaka and M. Tanaka, [18], presented a new method of solving the simplified energy equation to obtain the oil film temperature distribution easily. The energy equation is made discrete by means of the control volume method. They concluded that the thermohydrodynamic performance of two-lobe journal bearing predicted by this method is in a good agreement with the measured one, viscosity temperature index of lubricant and journal surface temperature have strong effects on the minimum oil film thickness and the maximum pad surface temperature.

S. A. Nassab and M. S. Moayeri, [19], presented analysis of the axially groove fluid film finite length journal bearing based on the thermohydrodynamic theory. Conformal mapping is used to generate an orthogonal grid and the governing equations are transformed in the computational domain. Discretized forms of the transformed equations are obtained by the control volume method and solved by the semi-implicit method. The numerical results were compared with several experimental data and a good agreement was found.

Jang and Khon Sari, [20], gave a very simple design procedure which enables one to rapidly predict the maximum bearing temperature, the shaft temperature and other bearing design parameters. They used two dimensionless temperature rise parameters to characterize the thermal behavior of a steady state hydrodynamic bearings.

From the above review, thermal behavior was primarily limited to employ a specific value of the viscosity, called effective viscosity, according to the average temperature rise in the oil film. This method did not provide any information about the maximum temperature. Adiabatic solution was used including variable viscosity and a simple energy equation uncoupled with Reynold's equation, this method can provide a rough value of maximum temperature. For more accurate, the present work represent an attempt to apply the thermohydrodynamic analysis for the journal bearing to study the thermal behavior for bearing of cement mill.

MATHEMATICAL MODEL AND THEORY

Viscosity of oil significantly affects the load carrying capacity of the bearings. Viscosity of oil decreases exponentially with an increase in temperature as a result, the load carrying capacity decreases as viscosity decreases. Several equations have been used to describe the viscosity temperature relation.

Thermohydrodynamic analysis of a bearing refers to a realistic solution of Reynolds' equation in which viscosity field is predicted based on the

computation of temperature field obtained from energy equation. Predictions of the bearing performance parameters based on thermohydrodynamic analysis requires simultaneous solution of the Reynold's equation (pressure field) coupled with the energy equation (temperature field) and the heat conduction equation (temperature field through the solids) through the equation related to the viscosity and temperature. In this chapter the main governing equations with appropriate boundary conditions required to solve the problem have been developed.

The global coordinates system that is used in the oil film is the fixed Cartesian coordinates system (x,y,z) . The original point is the contact point of the journal bearing line centers with the inner ring of the bearing bush, the (y)

coordinate matches the line centers, the (x) coordinate is in the rotation direction, and the (z) coordinate is perpendicular to the (x,y) plane as shown in

figure (3-1). The non-dimensional coordinates $(\bar{x}, \bar{y}, \bar{z})$ are used to solve the governing equations. The (θ, r) coordinates are used to describe the temperature through the solid bodies (shaft and bearing bush).

Where:

$$\bar{x} = \frac{x}{R} : \text{coordinate in circumferential direction}$$

$$\bar{y} = \frac{y}{h} : \text{coordinate in the oil film thickness direction}$$

$$\bar{z} = \frac{z}{L} : \text{coordinate in axial direction}$$

$$\bar{r} = \begin{cases} \frac{r_b}{r_{bin}} : \text{radial coordinate in radial direction for the bearing} \\ \\ \frac{r_s}{R} : \text{radial coordinate in radial direction for the shaft} \end{cases}$$

The fluid film forces are obtained by solving the basic lubrication equation for pressure distribution which so called Reynold's equation. Reynold's equation with variable viscosity is derived as shown in Appendix (A).

The dimensionless form of this equation with variable viscosity reported by [12] as:

$$\frac{\partial}{\partial \bar{x}} \left(\bar{F} \bar{h}^3 \frac{\partial \bar{P}}{\partial \bar{x}} \right) + \left(\frac{R}{L} \right)^2 \frac{\partial}{\partial \bar{z}} \left(\bar{F} \bar{h}^3 \frac{\partial \bar{P}}{\partial \bar{z}} \right) = \frac{\partial}{\partial x} \left(\bar{G} \bar{h} \right) \quad \dots\dots\dots(3.1)$$

Where:

$$\bar{F} = \frac{\int_0^1 \left(\int_0^{\bar{y}} \frac{1}{\bar{\mu}} d\bar{y} \int_0^{\bar{y}} \frac{1}{\bar{\mu}} d\bar{y} - \int_0^{\bar{y}} \frac{1}{\bar{\mu}} d\bar{z} \int_0^{\bar{y}} \frac{1}{\bar{\mu}} d\bar{y} \right) d\bar{y}}{\int_0^1 \frac{1}{\bar{\mu}} d\bar{y}} \quad \dots\dots\dots(3.2)$$

$$\bar{G} = \frac{\int_0^1 \left(\int_0^{\bar{y}} \frac{1}{\bar{\mu}} d\bar{y} \right) d\bar{y}}{\int_0^1 \frac{1}{\bar{\mu}} d\bar{y}} \quad \dots\dots\dots(3.3)$$

$$\bar{h} = \frac{h}{c} \quad \bar{x} = \frac{x}{R} \quad \bar{y} = \frac{y}{h} \quad \bar{z} = \frac{z}{L} \quad \bar{\mu} = \frac{\mu}{\mu_{in}}$$

The oil film thickness can be evaluated as described by [34] as:

$$\bar{h} = \frac{h}{c} = \lambda + \varepsilon \cos \bar{x} \quad \dots\dots\dots(3.4)$$

The dimensionless form of the oil-film velocity components ($\bar{u}, \bar{v}, \bar{w}$) in ($\bar{x}, \bar{y}, \bar{z}$) directions were described by [35] as:

$$\bar{u} = \frac{\partial \bar{p}}{\partial \bar{x}} \bar{h}^2 \left(- \frac{\int_0^{\bar{y}} \frac{1}{\bar{\mu}} d\bar{y} \int_0^{\bar{y}} \frac{1}{\bar{\mu}} d\bar{y}}{\int_0^1 \frac{1}{\bar{\mu}} d\bar{y}} + \int_0^{\bar{y}} \frac{1}{\bar{\mu}} d\bar{y} \right) + \frac{\int_0^{\bar{y}} \frac{1}{\bar{\mu}} d\bar{y}}{\int_0^1 \frac{1}{\bar{\mu}} d\bar{y}} \quad \dots\dots\dots(3.5)$$

$$\bar{w} = \frac{\partial \bar{p}}{\partial z} \bar{h}^2 \left(\frac{R}{L} \right) \left(\int_0^{\bar{y}} \frac{\bar{y}}{\mu} d\bar{y} - \frac{\int_0^1 \frac{\bar{y}}{\mu} d\bar{y} \int_0^{\bar{y}} \frac{1}{\mu} d\bar{y}}{\int_0^1 \frac{1}{\mu} d\bar{y}} \right) \quad \dots(3.6)$$

$$\bar{v} = -\bar{h} \int_0^{\bar{y}} \left\{ \frac{\partial \bar{u}}{\partial x} + \left(\frac{R}{L} \right) \frac{\partial \bar{w}}{\partial z} - \frac{\bar{y}}{h} \frac{\partial \bar{h}}{\partial x} \frac{\partial \bar{u}}{\partial y} \right\} d\bar{y} \quad \dots(3.7)$$

Where:

$$\bar{u} = \frac{u}{U} \quad \bar{w} = \frac{w}{U} \quad \bar{v} = \frac{v}{U} \left(\frac{R}{c} \right) \quad \dots(3.8)$$

3.3

Energy equation

The following assumptions are made in deriving the energy equation:-

- 1- The lubricant density and thermal conductivity remain constant.
- 2- Heat conduction for the lubricant in the direction of sliding motion of the bearing surface is neglected since it is small compared with the heat convection in the same direction [11].
- 3- The axial variation in temperature can be ignored as being small [12, 13, and 14].

The above assumptions lead to the energy equation such that given by

[15, and 16].

The dimensionless form of the energy equation is given as:-

$$\lambda_1 \bar{u} \frac{\partial \bar{t}}{\partial \bar{x}} + \lambda_1 \left(\frac{\bar{v}}{\bar{h}} - \bar{u} \frac{\bar{y}}{\bar{h}} \frac{\partial \bar{h}}{\partial \bar{x}} \right) \frac{\partial \bar{t}}{\partial \bar{y}} = \frac{1}{\bar{h}^2} \lambda_2 \frac{\partial^2 \bar{t}}{\partial \bar{y}^2} + \frac{\bar{\mu}}{\bar{h}^2} \lambda_3 \left[\left(\frac{\partial \bar{u}}{\partial \bar{y}} \right)^2 + \left(\frac{\partial \bar{w}}{\partial \bar{y}} \right)^2 \right] \quad \dots(3.9)$$

Where:

$$\lambda_1 = \frac{\rho U C_o R}{k_{oil}} \quad \dots(3.10)$$

$$\lambda_2 = \left(\frac{R}{c} \right)^2 \quad \dots(3.11)$$

$$\lambda_3 = \left(\frac{R}{c} \right)^2 \frac{\mu_i U^2}{k_{oil} t_{in}} \quad \dots(3.12)$$

The dimensionless oil temperature is:

$$\bar{t} = \frac{t}{t_{in}} \quad \dots(3.13)$$

A full derivation for the energy equation can be found in appendix B.

3.4

Heat conduction equation

The temperature distribution through the soled boundaries (journal and bearing) can be evaluated by solving the heat conduction equation. The steady state heat conduction equation with no heat source can be written as^[7]:-

$$\frac{\partial^2 \bar{t}}{\partial \bar{r}^2} + \frac{1}{\bar{r}} \frac{\partial \bar{t}}{\partial \bar{r}} + \frac{1}{\bar{r}^2} \frac{\partial^2 \bar{t}}{\partial \theta^2} = 0 \quad \dots(3.14)$$

The viscosity of the lubricant was assumed to be variable across the film and around the circumference. The relationship between the viscosity and the temperature is given by the following equation as described by [۲]:

$$\bar{\mu} = k_0 - k_1 \bar{t} + k_2 \bar{t}^2 \quad \dots(۳.۱۵)$$

where:

k_0, k_1, k_2 the lubricant viscosity coefficients.

The attitude angle (ϕ) can be written by the relation as described by [۲]:

$$\phi = \tan^{-1} \left(-\frac{\bar{w}_i}{\bar{w}_r} \right) \quad \dots(۳.۱۶)$$

Where \bar{w}_r and \bar{w}_i are the components of dimensionless load in the direction of line of centers of the journal and the normal to the line which can be evaluated as:

$$\bar{w}_r = \int_0^1 \int_0^{2\pi} \bar{p} \cos \bar{x} d\bar{x} d\bar{z} \quad \dots(3.17)$$

$$\bar{w}_i = \int_0^1 \int_0^{2\pi} \bar{p} \sin \bar{x} d\bar{x} d\bar{z} \quad \dots(3.18)$$

3.7

Boundary conditions

The following boundary conditions have been used with the above governing equation to achieve the thermohydrodynamic analysis of the bearing.

The boundary conditions which were used with the Reynolds' equation can be expressed as described by [12] as:-

At the oil supply groove $\bar{x} = 2\pi - \phi \quad \bar{p} = \bar{p}_s \quad \dots(3.19)$

At the journal bearing edges $\bar{z} = 0 \text{ and } \bar{z} = 1 \quad \bar{p} = \bar{p}_{atm} = 0.0 \quad \dots(3.20)$

At the cavitation zone $\frac{\partial \bar{p}}{\partial \bar{x}} = 0.0 \quad \bar{p} = 0.0 \quad \dots(3.21)$

The temperature distribution through the oil film can be determined by solving the energy equation subjected to the following boundary conditions :

- 1- The temperature across the oil film in the groove zone (t_{mix}) is assumed to be constant and can be estimated as described by [12, and 19] as follows:

$$t_{mix} = \frac{Q_{rec} t_r + Q_{in} t_{in}}{Q_{rec} + Q_{in}} \quad \dots(3.22)$$

ϒ- The heat flux continuity on the surface between the bush and the oil film is assumed to be valid at the bearing oil film interface which yields to the followed as described by [° ,and ١٢]:-

$$\left. \frac{\partial \bar{t}}{\partial \bar{r}} \right|_{\bar{r}=1} = - \frac{k_{oil}}{k_b} \frac{r_{bin}}{c} \frac{1}{h} \left. \frac{\partial \bar{t}}{\partial \bar{y}} \right|_{\bar{y}=0} \quad \dots(٣.٢٣)$$

where :

$$\bar{r} = \frac{r_b}{r_{bin}}$$

ϓ- For the shaft oil film interface, the temperature is given by the heat flux continuity assuming that the shaft temperature is independent on circumferential direction as described by [°, and ٩] this gives:

$$\left. \frac{\partial \bar{t}}{\partial \bar{r}} \right|_{\bar{r}=1} = - \frac{1}{2\pi} \frac{k_o}{k_s} \frac{R}{c} \int_0^{2\pi} \frac{1}{h} \left. \frac{\partial \bar{t}}{\partial \bar{y}} \right|_{\bar{y}=1} d\bar{x} \quad \dots(٣.٢٤)$$

where :

$$\bar{r} = \frac{r_s}{R}$$

ξ- The temperature distribution through the stationary solid is determined by solving the Laplace heat conduction equation subjected to the following boundary condition which was referred to the loses heat by free convection[٩]:

$$\left. \frac{\partial \bar{t}}{\partial \bar{r}} \right|_{\bar{r}=r_{bout}} = - \frac{h_{conv}}{k_b} r_{bin} \left(\bar{t}_{bo} - \bar{t}_a \right) \quad \dots(٣.٢٥)$$

The dimensionless governing equations are discretized and solved by using the finite difference method to get the pressure and the temperature distribution in the oil film and the bearing body. A suitable numerical method was used to solve the differential equations. The successive under relaxation method was used, in this method the rate of convergence of the iteration can be accelerated. A computer program written in a suitable scientific language (Fortran ۹۰).

The solution of system of partial differential equations can be greatly simplified by a well – constructed grid. The dimensionless oil film pressure distribution (\bar{p}) can be obtained by solving equation (۳.۱). The equation is

discretized yielding the mesh size of (n) in circumferential direction, (jj) across the oil film thickness and (kk) along the length of the bearing. For bearing bush and the shaft, the mesh size of (ss) in radial direction, has been used. In the present analysis (۳۶۰) divisions in the circumferential direction, (۶) divisions across the oil film thickness, (۲۰) divisions in the axial direction, and (۸) divisions in the radial direction have been adopted, and as are shown in figures (۳-۲) and (۳-۳).

The mesh size in circumferential direction can be defined as:

$$\Delta x = \frac{2\pi R}{n} \quad \dots(3.26)$$

which can be normalized as:-

$$\bar{\Delta x} = \frac{\Delta x}{R} \quad \dots(3.27)$$

Through the oil film thickness the oil film can be divided to slices of thickness Δy as follows:-

$$\Delta y = \frac{h}{jj} \quad \dots(3.28)$$

which can be normalized as:-

$$\bar{\Delta y} = \frac{\Delta y}{h} \quad \dots(3.29)$$

The bearing can be divided in axial direction to kk steps of width Δz as follows:-

$$\Delta z = \frac{L}{kk} \quad \dots(3.30)$$

Which can be normalized as:-

$$\bar{\Delta z} = \frac{\Delta z}{L} \quad \dots(3.31)$$

The bearing bush can be divided radially to many layers, each layer of thickness Δr as follows:-

$$\Delta r = \frac{(r_{bout} - r_{bin})}{ss} \quad \dots(3.32) \text{ it}$$

can be normalized as:-

$$\Delta \bar{r} = \frac{\Delta r}{r_{bin}} \quad \dots(3.33)$$

while the mesh size on the bearing shaft in radial direction can be evaluated as

$$\Delta \bar{r} = \frac{\Delta r}{R} \quad \dots(3.34)$$

The mesh size in circumferential direction in the bush can be defined as:

$$\Delta \theta = \frac{2\pi}{ss} \quad \dots(3.35)$$

3.8.2

Reynold's Equation

Reynold's equation is made discrete at the spaced grid points in the coordinates $(\bar{x}, \bar{y}, \bar{z})$ to make it suitable for the finite difference method in order to gate the pressure distribution (\bar{P}) through the oil film. Discretized equation discretized yielding the mesh size of (n) in circumferential direction, (jj) across the oil film thickness (kk) across the width of the bearing. Hence the discrete from the Reynold's equation can be written as:-

$$\frac{\partial \bar{p}}{\partial \bar{x}} \left(3\bar{h}^{-2} \bar{F} \frac{\partial \bar{h}}{\partial \bar{x}} + \bar{h}^{-3} \frac{\partial \bar{F}}{\partial \bar{x}} \right) + \bar{F} \bar{h}^{-3} \frac{\partial^2 \bar{p}}{\partial \bar{x}^2} + \left(\frac{R}{L} \right)^2 \bar{F} \bar{h}^{-3} \frac{\partial^2 \bar{p}}{\partial \bar{z}^2} = \bar{h} \frac{\partial \bar{G}}{\partial \bar{x}} + \bar{G} \frac{\partial \bar{h}}{\partial \bar{x}} \quad \dots(3.36)$$

$$3\bar{h}^{-2} \bar{F} \frac{\partial \bar{p}}{\partial \bar{x}} \frac{\partial \bar{h}}{\partial \bar{x}} + \bar{h}^{-3} \frac{\partial \bar{p}}{\partial \bar{x}} \frac{\partial \bar{F}}{\partial \bar{x}} + \bar{F} \bar{h}^{-3} \frac{\partial^2 \bar{p}}{\partial \bar{x}^2} + \left(\frac{R}{L} \right)^2 \bar{F} \bar{h}^{-3} \frac{\partial^2 \bar{p}}{\partial \bar{z}^2} = \bar{h} \frac{\partial \bar{G}}{\partial \bar{x}} + \bar{G} \frac{\partial \bar{h}}{\partial \bar{x}} \quad \dots(3.37)$$

For any point in the oil film mesh (i,j,k) :

$$\begin{aligned}
& 3\bar{h}_{i,k}^2 \bar{F}_{i,k} \frac{(\bar{P}_{i+1,k} - \bar{P}_{i,k}) (\bar{h}_{i+1,k} - \bar{h}_{i,k})}{(\Delta \bar{x})} + \bar{h}_{i,k}^3 \frac{(\bar{p}_{i+1,k} - \bar{p}_{i,k}) (\bar{F}_{i+1,k} - \bar{F}_{i,k})}{(\Delta \bar{x})} \\
& + \bar{F}_{i,k} \bar{h}_{i,k}^3 \frac{(\bar{p}_{i+1,k} - 2\bar{p}_{i,k} + \bar{p}_{i-1,k})}{(\Delta \bar{x})^2} + \left(\frac{R}{L}\right)^2 \bar{h}_{i,k}^3 \bar{F}_{i,k} \frac{(\bar{p}_{i,k+1} - 2\bar{p}_{i,k} + \bar{p}_{i,k-1})}{(\Delta \bar{z})^2} \quad \dots (3.38) \\
& = \bar{h}_{i,k} \frac{(\bar{G}_{i+1,j} - \bar{G}_{i,j})}{(\Delta \bar{x})} + \bar{G}_{i,j} \frac{(\bar{h}_{i+1,k} - \bar{h}_{i,k})}{(\Delta \bar{x})}
\end{aligned}$$

The equation can be written as :

$$\begin{aligned}
& 3\bar{h}_{i,k}^2 \bar{F}_{i,j} \bar{p}_{i+1,k} (\bar{h}_{i+1,k} - \bar{h}_{i,k}) (\Delta \bar{z})^2 + \bar{h}_{i,k}^3 \bar{p}_{i+1,k} (\bar{F}_{i+1,j} - \bar{F}_{i,j}) (\Delta \bar{z})^2 + \bar{F}_{i,j} \bar{h}_{i,k}^3 \bar{p}_{i+1,k} (\Delta \bar{z})^2 + \\
& \bar{F}_{i,j} \bar{h}_{i,k}^3 \bar{p}_{i-1,k} (\Delta \bar{z})^2 + \left(\frac{R}{L}\right)^2 \bar{h}_{i,k}^3 \bar{F}_{i,j} (\bar{p}_{i,k+1} + \bar{p}_{i,k-1}) (\Delta \bar{x})^2 = \bar{p}_{i,k} 3\bar{h}_{i,k}^2 \bar{F}_{i,j} (\bar{h}_{i+1,k} - \bar{h}_{i,k}) (\Delta \bar{z})^2 + \\
& \bar{h}_{i,k}^3 \bar{p}_{i,k} (\bar{F}_{i+1,j} - \bar{F}_{i,j}) (\Delta \bar{z})^2 + 2\bar{p}_{i,k} \bar{F}_{i,j} \bar{h}_{i,k}^3 (\Delta \bar{z})^2 + 2\bar{p}_{i,k} \left(\frac{R}{L}\right)^2 \bar{h}_{i,k}^3 \bar{F}_{i,j} (\Delta \bar{x})^2 + \bar{h}_{i,k} \\
& (\bar{G}_{i+1,j} - \bar{G}_{i,j}) \Delta \bar{x} (\Delta \bar{z})^2 + \bar{G}_{i,j} (\bar{h}_{i+1,k} - \bar{h}_{i,k}) \Delta \bar{x} (\Delta \bar{z})^2 \quad \dots (3.39)
\end{aligned}$$

which can be rearranged and rewritten as follows:

$$\begin{aligned}
\bar{p}_{i,k} & = [\bar{p}_{i+1,k} \{3\bar{h}_{i,k}^2 \bar{F}_{i,j} (\Delta \bar{z})^2 (\bar{h}_{i+1,k} - \bar{h}_{i,k}) + \bar{h}_{i,k}^3 (\Delta \bar{z})^2 (\bar{F}_{i+1,j} - \bar{F}_{i,j}) + \bar{F}_{i,j} \bar{h}_{i,k}^3 (\Delta \bar{z})^2\} + \\
& \bar{p}_{i-1,k} \{\bar{F}_{i,j} \bar{h}_{i,k}^3 (\Delta \bar{z})^2\} + \bar{p}_{i,k+1} \left\{\left(\frac{R}{L}\right)^2 \bar{h}_{i,k}^3 \bar{F}_{i,j} (\Delta \bar{x})^2\right\} + \bar{p}_{i,k-1} \left\{\left(\frac{R}{L}\right)^2 \bar{h}_{i,k}^3 \bar{F}_{i,j} (\Delta \bar{x})^2 - \right. \\
& \left. \bar{G}_{i,j} (\Delta \bar{z})^2 \Delta \bar{x} \{(\bar{h}_{i+1,k} - \bar{h}_{i,k}) - \bar{h}_{i,k}\} - \bar{G}_{i+1,j} \bar{h}_{i,k} \Delta \bar{x} (\Delta \bar{z})^2\} / [3\bar{h}_{i,k}^2 \bar{F}_{i,j} (\bar{h}_{i+1,k} - \bar{h}_{i,k}) \right. \\
& \left. (\Delta \bar{z})^2 + \bar{h}_{i,k}^3 (\bar{F}_{i+1,j} - \bar{F}_{i,j}) (\Delta \bar{z})^2 + 2\bar{F}_{i,j} \bar{h}_{i,k}^3 (\Delta \bar{z})^2 + 2\left(\frac{R}{L}\right)^2 \bar{h}_{i,k}^3 \bar{F}_{i,j} (\Delta \bar{x})^2 \quad \dots (3.40)
\end{aligned}$$

The above equation can be simplified to get :

$$\begin{aligned} \bar{p}_{i,k} = & [\bar{p}_{i+1,k} \{3\bar{h}_{i,k}^2 \bar{F}_{i,j} (\Delta\bar{z})^2 \bar{h}_{i+1,k} - 3\bar{h}_{i,k}^3 \bar{F}_{i,j} (\Delta\bar{z})^2 - \bar{h}_{i,k}^3 \bar{F}_{i,j} (\Delta\bar{z})^2 + \bar{F}_{i+1,j} \bar{h}_{i,k}^3 (\Delta\bar{z})^2 + \bar{h}_{i,k}^3 \bar{F}_{i,j} (\Delta\bar{z})^2\} + \\ & \bar{p}_{i-1,k} \{\bar{F}_{i,j} \bar{h}_{i,k}^3 (\Delta\bar{z})^2\} + \bar{p}_{i,k+1} \{(\frac{R}{L})^2 \bar{h}_{i,k}^3 \bar{F}_{i,j} (\Delta\bar{x})^2\} + \bar{p}_{i,k-1} \{(\frac{R}{L})^2 \bar{h}_{i,k}^3 \bar{F}_{i,j} (\Delta\bar{x})^2\} + \\ & \bar{G}_{i,j} \{(\Delta\bar{z})^2 (\Delta\bar{x}) (2\bar{h}_{i,k} - \bar{h}_{i+1,k})\} - \bar{G}_{i+1,j} \{\bar{h}_{i,k} (\Delta\bar{x}) (\Delta\bar{z})^2\}] / [-3\bar{h}_{i,k}^3 \bar{F}_{i,j} (\Delta\bar{z})^2 - \bar{h}_{i,k}^3 \bar{F}_{i,j} (\Delta\bar{z})^2 + \\ & 2\bar{h}_{i,k}^3 \bar{F}_{i,j} (\Delta\bar{z})^2 + 3\bar{h}_{i,k} \bar{h}_{i+1,k} \bar{F}_{i,j} (\Delta\bar{z})^2 + \bar{h}_{i,k}^3 \bar{F}_{i+1,j} (\Delta\bar{z})^2 + 2(\frac{R}{L})^2 \bar{h}_{i,k}^3 \bar{F}_{i,j} (\Delta\bar{x})^2] \quad \dots(\text{૩.૧૧}) \end{aligned}$$

Which can be rearranged as:-

$$A1 = \bar{p}_{i+1,k} \bar{h}_{i,k}^2 (\Delta\bar{z})^2 (3\bar{F}_{i,j} \bar{h}_{i,k} - 3\bar{h}_{i,k} \bar{F}_{i,j} + \bar{h}_{i,k} \bar{F}_{i+1,j}) \quad \dots(\text{૩.૧૨})$$

$$A2 = \bar{p}_{i-1,k} \bar{h}_{i,k}^3 \bar{F}_{i,j} (\Delta\bar{z})^2 \quad \dots(\text{૩.૧૩})$$

$$A3 = \bar{p}_{i,k+1} \bar{h}_{i,k}^3 \bar{F}_{i,j} (\frac{R}{L})^2 (\Delta\bar{x})^2 \quad \dots(\text{૩.૧૪})$$

$$A4 = \bar{p}_{i,k-1} \bar{h}_{i,k}^3 \bar{F}_{i,j} (\frac{R}{L})^2 (\Delta\bar{x})^2 \quad \dots(\text{૩.૧૫})$$

$$A5 = \bar{G}_{i,j} (\Delta\bar{x}) (\Delta\bar{z})^2 (\bar{h}_{i+1} - \bar{h}_i) \quad \dots(\text{૩.૧૬})$$

$$A6 = \bar{h}_{i,k} (\Delta\bar{x}) (\Delta\bar{z})^2 (\bar{G}_{i+1,j} - \bar{G}_{i,j}) \quad \dots(\text{૩.૧૭})$$

$$A11 = 3\bar{h}_{i,k}^2 \bar{F}_{i,j} (\Delta\bar{z})^2 (\bar{h}_{i+1,k} - \bar{h}_{i,k}) \quad \dots(\text{૩.૧૮})$$

$$A22 = 2\bar{h}_{i,k}^3 \bar{F}_{i,j} (\Delta\bar{z})^2 \quad \dots(\text{૩.૧૯})$$

$$A33 = 2\bar{h}_{i,k}^3 \bar{F}_{i,j} (\frac{R}{L})^2 (\Delta\bar{x})^2 \quad \dots(\text{૩.૨૦})$$

$$A44 = \bar{h}_{i,k}^3 (\Delta\bar{z})^2 (\bar{F}_{i+1,j} - \bar{F}_{i,k}) \quad \dots(\text{૩.૨૧})$$

Then the last form of the equation as:-

$$\bar{p}_{i,k} = \frac{A1 + A2 + A3 + A4 + A5 + A6}{A11 + A22 + A33 + A44} \quad \dots(3.02)$$

The above equation gives the dimensionless oil film pressure in the circumference and axial directions

3.8.3

The energy equation

Energy equation is made discrete in the (\bar{x}, \bar{y}) plane to get the dimensionless oil film temperature along the circumferential and across the oil film as follows:-

$$\lambda_1 \bar{u}_{(i,j)} \frac{\bar{t}_{(i,j)} - \bar{t}_{(i-1,j)}}{(\Delta \bar{x})} + \lambda_1 \left[\frac{\bar{v}_{(i,j)}}{\bar{h}_{(i,k)}} - \bar{u}_{(i,j)} \frac{\bar{y}_{(i,j)} (\bar{h}_{(i,k)} - \bar{h}_{(i-1,k)})}{\bar{h}_{(i,k)} (\Delta \bar{x})} \right] \left[\frac{\bar{t}_{(i,j)} - \bar{t}_{(i,j-1)}}{(\Delta \bar{y})} \right] = \dots(3.03)$$

$$\frac{1}{\bar{h}_{(i,k)}} \lambda_2 \frac{\bar{t}_{(i,j+1)} - 2\bar{t}_{(i,j)} + \bar{t}_{(i,j-1)}}{(\Delta \bar{y})^2} + \frac{\bar{\mu}_{(i,j)}}{\bar{h}_{(i,k)}} \lambda_2 \left[\left(\frac{\bar{u}_{(i,j)} - \bar{u}_{(i,j-1)}}{\Delta \bar{y}} \right)^2 + \left(\frac{\bar{w}_{(i,j)} - \bar{w}_{(i,j-1)}}{\Delta \bar{y}} \right)^2 \right]$$

..

The above equation can be simplified by multiplying both sides by $\Delta \bar{x} \Delta \bar{y}^2 \bar{h}^{-2}$ to get:

$$\lambda_1 \bar{u}_{(i,j)} \left(\Delta \bar{y} \right)^2 \left(\bar{t}_{(i,j)} - \bar{t}_{(i-1,j)} \right) \bar{h}^2_{(i,k)} + \lambda_1 \bar{h}_{(i,k)} \left(\Delta \bar{y} \right) \left(\bar{v}_{(i,j)} * \Delta \bar{x} - \bar{u}_{i,j} \bar{y}_{i,j} \left(\bar{h}_{(i+1,k)} - \bar{h}_{(i,k)} \right) \right) * \left(\bar{t}_{(i,j)} - \bar{t}_{(i,j-1)} \right) = \lambda_2 \left(\Delta \bar{x} \right) \left(\bar{t}_{(i,j+)} - 2\bar{t}_{(i,j)} + \bar{t}_{(i,j-)} \right) + \bar{\mu}_{i,j} \lambda_3 \Delta \bar{x} \left(\left(\bar{u}_{(i,j)} - \bar{u}_{(i,j-1)} \right)^2 + \left(\bar{w}_{(i,j)} - \bar{w}_{(i,j-1)} \right)^2 \right) \dots(3.54)$$

which can be rearranged and rewritten as follows:

$$\bar{t}_{(i,j)} \left(\lambda_1 \bar{u}_{(i,j)} \left(\Delta \bar{y} \right)^2 \bar{h}^2_{(i,k)} + \lambda_1 \bar{h}_{(i,k)} \left(\Delta \bar{y} \right) \left(\bar{v}_{(i,j)} \Delta \bar{x} - \bar{u}_{(i,j)} \bar{y}_{(i,j)} \left(\bar{h}_{(i,k)} - \bar{h}_{(i-1,k)} \right) \right) + 2\lambda_2 \left(\Delta \bar{x} \right) \right) = \bar{t}_{(i-1,j)} \left(\lambda_1 \bar{h}_{(i,k)} \left(\Delta \bar{y} \right)^2 \bar{h}^2_{(i,k)} \right) + \bar{t}_{(i,j-1)} \left(\lambda_1 \bar{h}_{(i,k)} \left(\Delta \bar{y} \right) \left(\bar{v}_{(i,j)} \Delta \bar{x} - \bar{u}_{(i,j)} \bar{y}_{(i,j)} \left(\bar{h}_{(i,k)} - \bar{h}_{(i-1,k)} \right) \right) \right) + \bar{t}_{(i,j+1)} \lambda_2 \left(\Delta \bar{x} \right) + \bar{t}_{(i,j-1)} \lambda_2 \left(\Delta \bar{x} \right) + \bar{\mu}_{i,j} \lambda_3 \left(\Delta \bar{x} \right) \left(\left(\bar{u}_{(i,j)} - \bar{u}_{(i,j-1)} \right)^2 + \left(\bar{w}_{(i,j)} - \bar{w}_{(i,j-1)} \right)^2 \right) \dots(3.55)$$

The dimensionless oil film temperature can be estimated as :

$$\bar{t}_{(i,j)} = \frac{\bar{t}_{(i-1,j)} \lambda_{11} + \bar{t}_{(i,j-1)} (\lambda_{12} + \lambda_{22}) + \bar{t}_{(i,j+1)} \lambda_{22} + \lambda_{33}}{\lambda_{11} + \lambda_{12} + \lambda_{22}} \dots(3.56)$$

Where :

$$\lambda_{11} = \lambda_1 \bar{u}_{(i,j)} (\Delta \bar{y}) \bar{h}^2_{i,k} \dots(3.57)$$

$$\lambda_{12} = \lambda_1 \bar{h}_{i,k} (\Delta \bar{y}) \{ \bar{v}_{i,j} \Delta \bar{x} - \bar{u}_{i,j} \bar{y}_{i,j} (\bar{h}_{i,k} - \bar{h}_{i-1,k}) \} \dots(3.58)$$

$$\lambda_{22} = \lambda_2 \Delta \bar{x} \dots(3.59)$$

$$\lambda_{33} = \bar{\mu}_{i,j} \lambda_3 \Delta \bar{x} \{ (\bar{u}_{i+1,j} - \bar{u}_{i,j})^2 + (\bar{w}_{i+1,j} - \bar{w}_{i,j})^2 \} \dots(3.60)$$

For the bearing bush the heat-conduction equation form is :

$$\frac{\partial^2 \bar{t}_b}{\partial \bar{r}^2} + \frac{1}{\bar{r}} \frac{\partial \bar{t}_b}{\partial \bar{r}} + \frac{1}{\bar{r}^2} \frac{\partial^2 \bar{t}_b}{\partial \theta^2} = 0 \quad \dots(3.61)$$

Where :

$$\bar{t}_b = \frac{t_b}{t_{in}} \quad t_b = \text{Bearing bush temperature} \quad t_{in} = \text{oil inlet temperature}$$

$$\bar{r} = \frac{r_b}{r_{bin}} \quad r_b = \text{Bearing bush radius} \quad r_{bin} = \text{Bearing bush inner radius}$$

The heat-conduction equation is made discrete at the (θ, \bar{r}) coordinate to get the dimensionless bush temperature as below :

$$\frac{\bar{t}_{b(i,j+1)} - 2\bar{t}_{b(i,j)} + \bar{t}_{b(i,j-1)}}{(\Delta \bar{r})^2} + \frac{1}{\bar{r}_{(j)}} \frac{\bar{t}_{b(i,j+1)} - \bar{t}_{b(i,j)}}{(\Delta \bar{r})} + \frac{1}{\bar{r}_{(j)}^2} \frac{\bar{t}_{b(i+1,j)} - 2\bar{t}_{b(i,j)} + \bar{t}_{b(i-1,j)}}{(\Delta \theta)^2} = 0 \quad (3.62)$$

The above equation can be simplified to get :

$$\begin{aligned} & \bar{t}_{b(i,j+1)}(\Delta \theta)^2 \left(\bar{r}_{(j)}^2 + \bar{r}_{(j)} (\Delta \bar{r}) \right) + \bar{t}_{b(i,j-1)} \left((\Delta \theta)^2 \bar{r}_{(j)}^2 \right) + \bar{t}_{b(i+1,j)} (\Delta \bar{r})^2 + \bar{t}_{b(i-1,j)} (\Delta \bar{r})^2 \\ & = \bar{t}_{b(i,j)} \left(2(\Delta \theta)^2 \bar{r}_{(j)}^2 + (\Delta \theta)^2 (\Delta \bar{r}) \bar{r}_{(j)} + 2(\Delta \bar{r})^2 \right) \end{aligned} \quad (3.63)$$

which can be rearranged and rewritten as follows:-

$$\bar{t}_{b(i,j)} = \frac{\bar{t}_{b(i,j+1)} \left((\Delta\theta)^2 \left(\bar{r}_{(j)}^{-2} + \bar{r}_{(j)} \Delta\bar{r} \right) \right) + \bar{t}_{b(i,j-1)} \left((\Delta\theta)^2 \bar{r}_{(j)}^{-2} \right) + \bar{t}_{b(i+1,j)} \left(\Delta\bar{r} \right)^2 + \bar{t}_{b(i-1,j)} \left(\Delta\bar{r} \right)^2}{2(\Delta\theta)^2 \bar{r}_{(j)}^{-2} + 2(\Delta\bar{r})^2 + (\Delta\theta)^2 \Delta\bar{r}\bar{r}_{(j)}}$$

.....(۳.۶۴)

The above equation gives the dimensionless bush temperature in the circumference and radial directions .

۳.۸.۵

Solution procedure

The temperature and pressure distribution in the oil film and solid parts

at the mid-plane of the journal bearing are obtained as follows:

۱-An initial value of the attitude angle (ϕ) is restricted as a first step in the solution procedure, which can be estimated depending on the classical

isothermal theory as[۳۳]:

$$\dots(۳.۶۵) \phi = \tan^{-1} \frac{\pi \sqrt{(1-\varepsilon^2)}}{4\varepsilon}$$

۲-The temperature of oil film, the bearing bush and the shaft grid points are assumed.

۳-The dimensionless value of the oil viscosity for all the points are computed by using the equation (۳.۱۵), after the estimation of the constants value (k_o, k_1, k_2)

for the used oil.

ξ-The dimensionless oil film thickness (\bar{h}) of the mid-plane of the journal is calculated from equation (3.4).

ο-Then the values of (\bar{F}, \bar{G}) are obtained by using the numerical integration (trapezoidal method) to solve equations (3.2) and (3.3).

ϒ-The initial value of oil pressure for all the grid points are assumed to have zero value except at the inlet zone when the value is assumed the inlet pressure value.

ϒ-An iterative scheme with successive under relaxation method is employed to solve equation (3.5) with the boundary conditions (3.19), (3.20) and (3.21) to obtain the dimensionless pressures of the oil film grid points which they are set at zero value for the negative pressures during the computation of the equation. The iterations are stopped when the converging criteria for the pressure equation, which can be calculated from the bellow equation, reach to (10^{-4}).

$$\dots(3.66) \in \bar{p} = \frac{\sum \sum \left| \bar{p}_{i,k}^n - \bar{p}_{i,k}^{n-1} \right|}{\sum \sum \left| \bar{p}_{i,k}^n \right|} < 10^{-4}$$

ϒ-After equations (3.17, 3.18) have been solved by using numerical integration technique, a new value of the attitude angle is computed from equation (3.16) and compared with an old one, the solution procedure is repeated by using the

new value of the attitude angle until the difference between the angles of the last two steps are reached less than one degree.

9-The dimensionless values of the fluid velocities ($\bar{u}, \bar{v}, \bar{w}$) are calculated according to equations (3.9), (3.6), and (3.7).

10-The values of the recirculation flow rate (Q_{rec}) and leakage flow rate (Q_l) are evaluated as follows:

The recirculation flow rate (Q_{rec}) for any section can be evaluated from the below integration.

$$Q_{rec} = L \int_0^h \bar{u} dy \quad \dots(3.67)$$

which can be rearranged as follows:

$$Q_{rec} = L U c \int_0^1 \bar{u} h d \bar{y} \quad \dots(3.68)$$

The leakage flow rate (Q_l) from the two edges of the journal bearing can be determined from:

$$Q_l = \int_0^{2\pi R} \int_0^h \bar{w} dy dx \quad \dots(3.69)$$

which can be rearranged as follows:

$$Q_l = R U c \int_0^{2\pi} \int_0^1 \bar{w} y d \bar{x} \quad \dots(3.70)$$

Numerical integration is used to solve the above equations.

11-The mixed oil temperature in the inlet zone is computed from equation (3.22) and this temperature is used as an initial inlet temperature to solve the energy equation.

12-The energy equation (3.56) and the heat transfer equation at the solids (3.64) subjected to the boundary conditions (3.23),(3.24)and(3.25), the shaft can be treated as an isothermal component for a full journal bearing as[12,13], are solved simultaneously to get the temperature filed. The mixed oil temperature is used as an inlet temperature. They are solved by the successive under relaxation iteration technique.

13-The new oil-film temperature is used to compute a new viscosity field which is subsequently used to solve the Reynolds' equation and simultaneous solutions for the equations are obtained iteratively until the converging criteria of the temperatures for all points on the boundary between the oil film and the bush (inner bush face) for two successive iteration steps is less than (10^{-6}) .

$$\dots(3.71) \in \bar{t} = \frac{\sum \sum \left| \bar{t}_{i,j}^{(n)} - \bar{t}_{i,j}^{(n-1)} \right|}{\sum \sum \left| \bar{t}_{i,j}^{(n)} \right|} < 10^{-6}$$

14-The applied load is computed form the equation below after the equations (3-17,3-18) have been solved:

$$W = Ul\mu_{in} (R/c)^2 \sqrt{\bar{w}_r^2 + \bar{w}_t^2} \dots(3.72)$$

15- If error ratio of the applied load is less than 10^{-3} the solution moves to the

next step, other wise modifies the value of ε and returns to step 1.

16- The results are printed.

3.8.6

Solution procedure for partial journal bearing

The same above procedure is used to solve the equations in the case of the 120° partial arc journal bearing, as shown in figure(3-4), but the following

modifications must be used:

1- Instead of the boundary conditions (3-19) used:

$$\text{At } \bar{x} = 2\pi/3 - \phi \quad \bar{p} = 0.0 \quad \dots(3.73)$$

2- Instead of the boundary conditions (3-21) used:

$$\text{At } \bar{x} = 4\pi/3 - \phi \quad \bar{p} = 0.0 \quad \dots(3.74)$$

3- Instead of the equation (3-22) used:

$$\text{At } \bar{x} = 2\pi/3 - \phi \quad t_{mix} = t_{in} \quad \dots(3.75)$$

3.9

Computer program

A suitable computer program was prepared and written in (FORTRAN – 90) language , to solve governing equations which govern the

performance of the journal bearing. The flow chart of the computer program can be shown in figure (3-6).

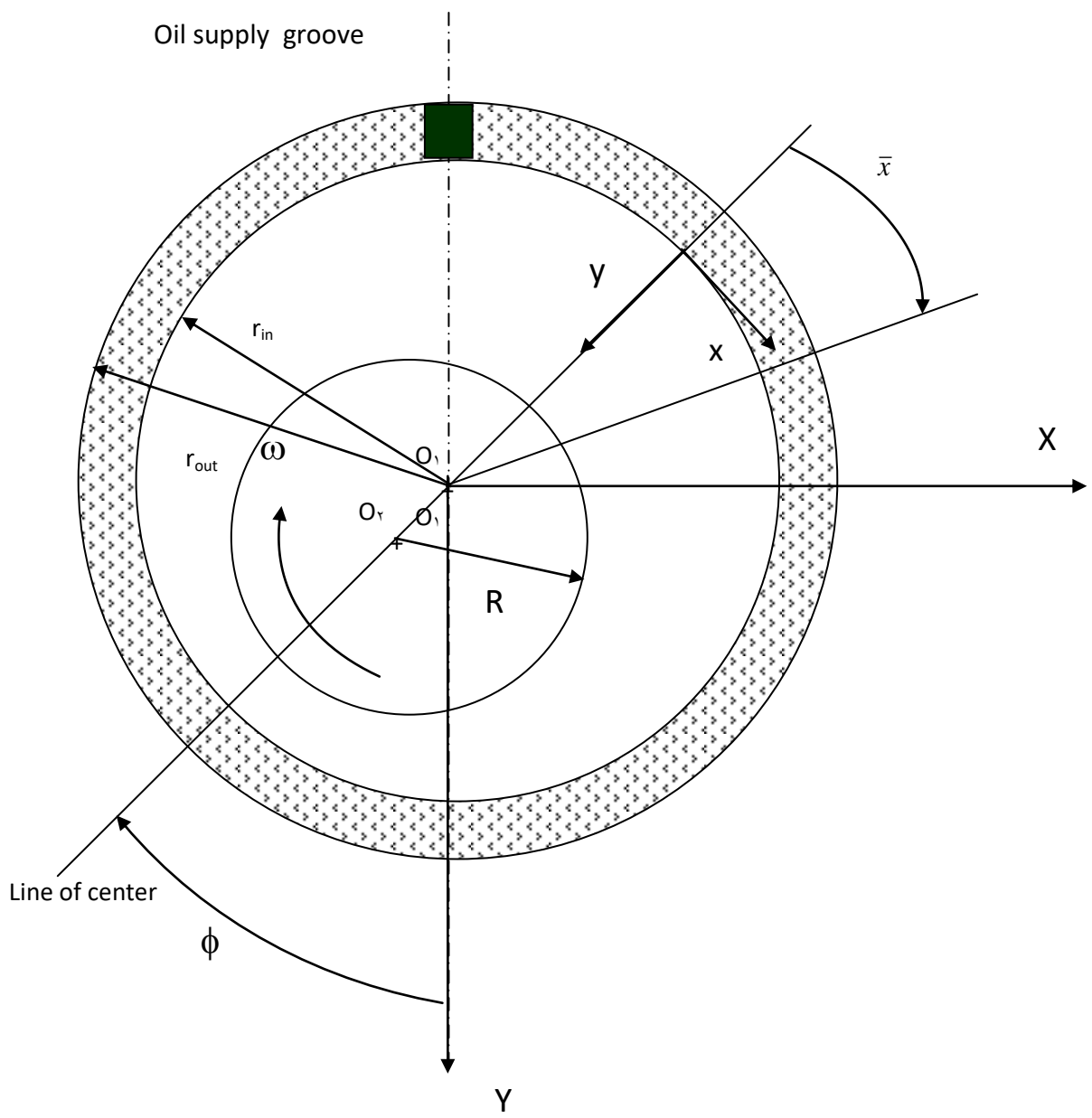


Fig.(3-1) Geometry of Journal Bearing and Coordinate System

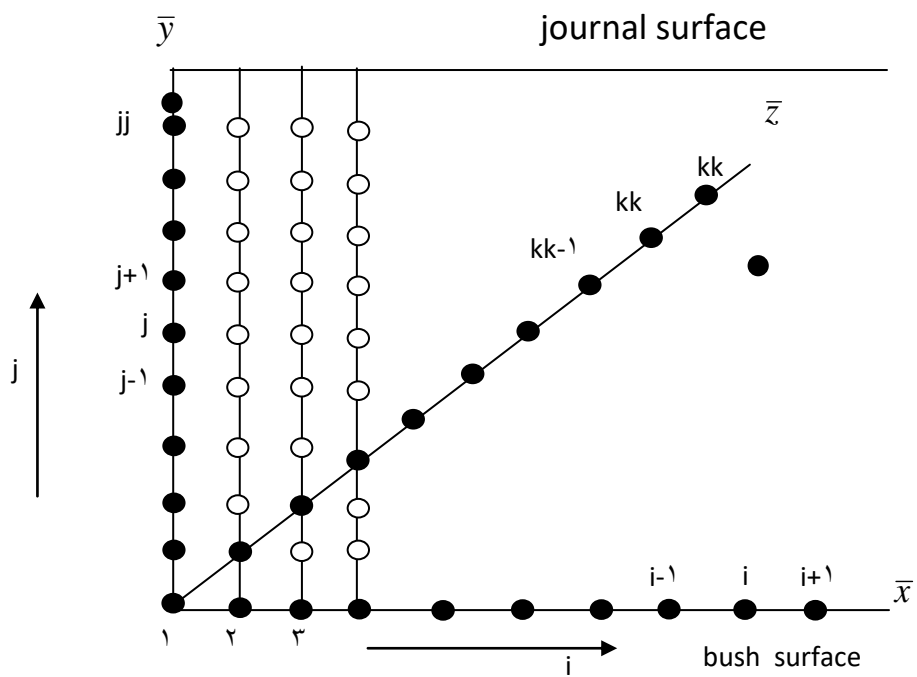


Fig.(۳-۲) Grid generation for oil film of journal bearing

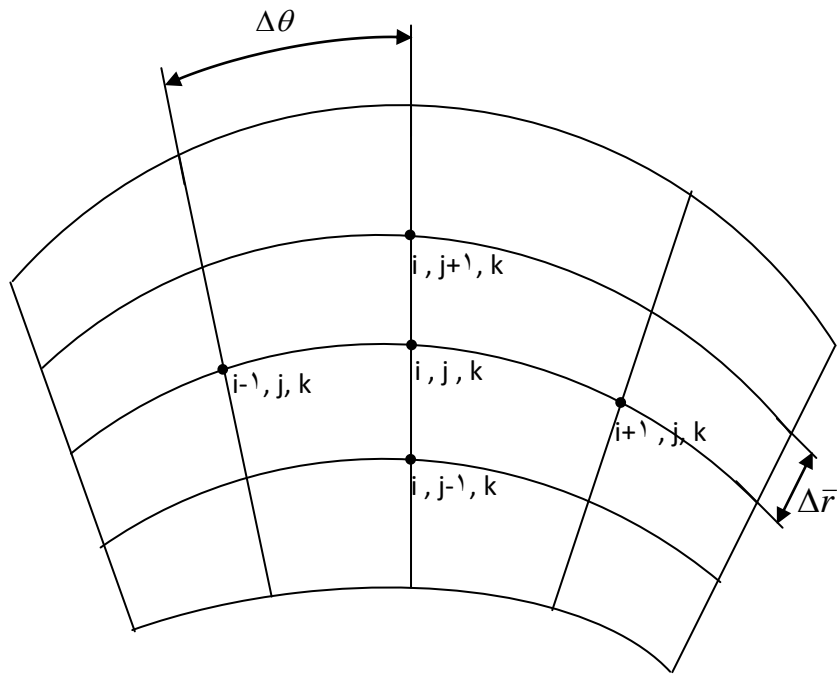
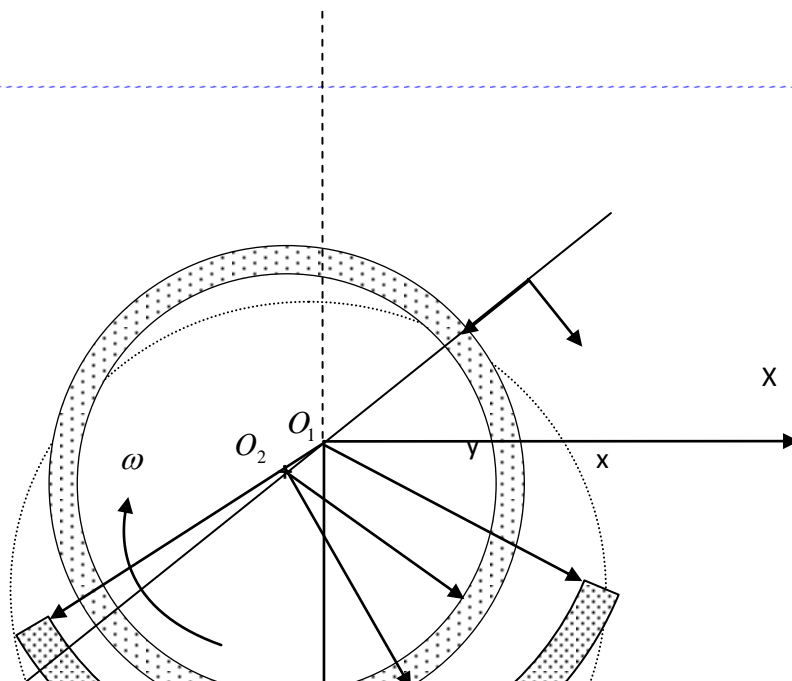


Fig.(3-3) Finite different grid for bearing bush



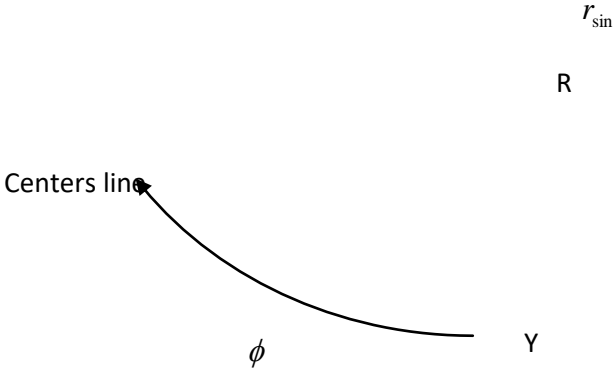


Fig.(3-4) Partial journal bearing

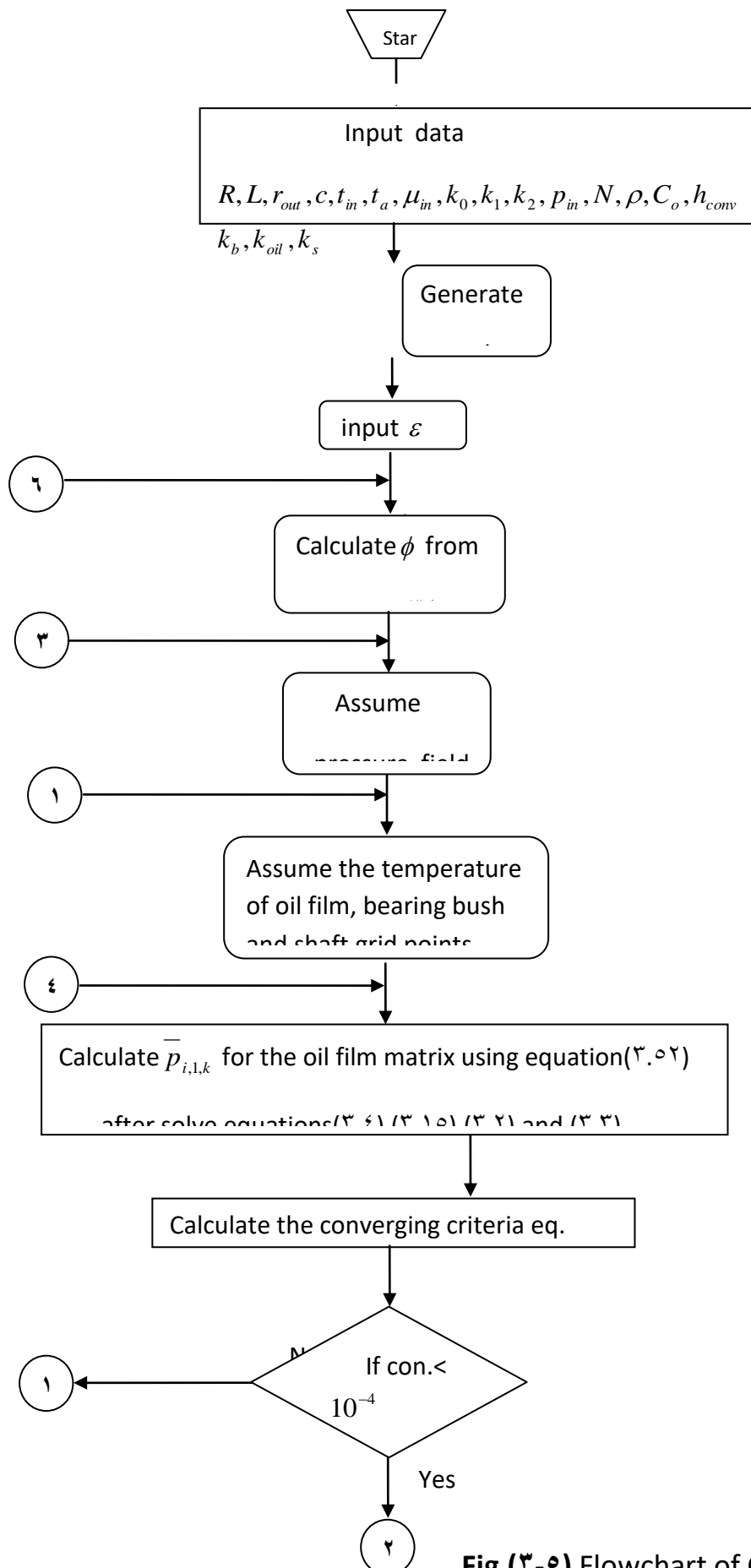
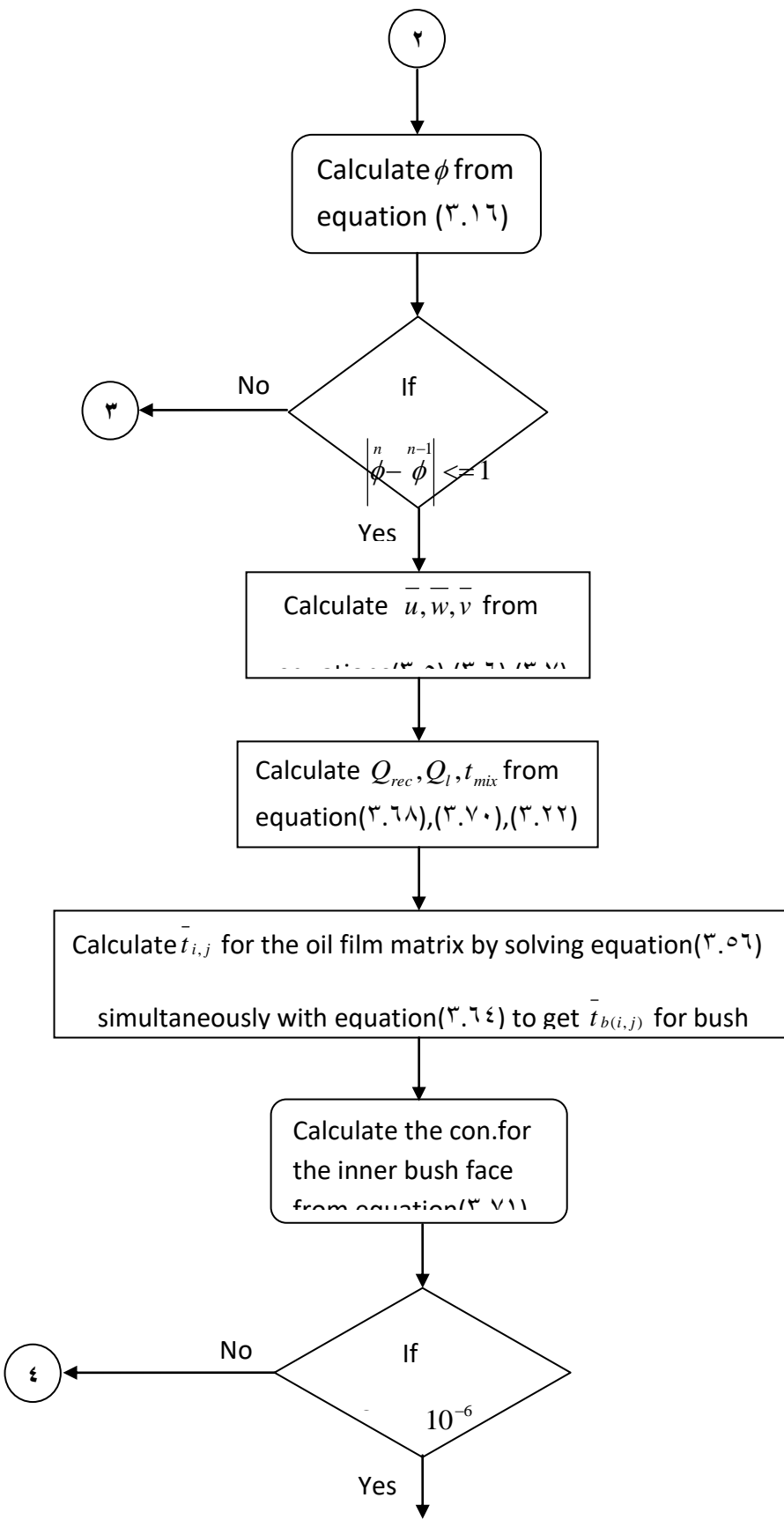
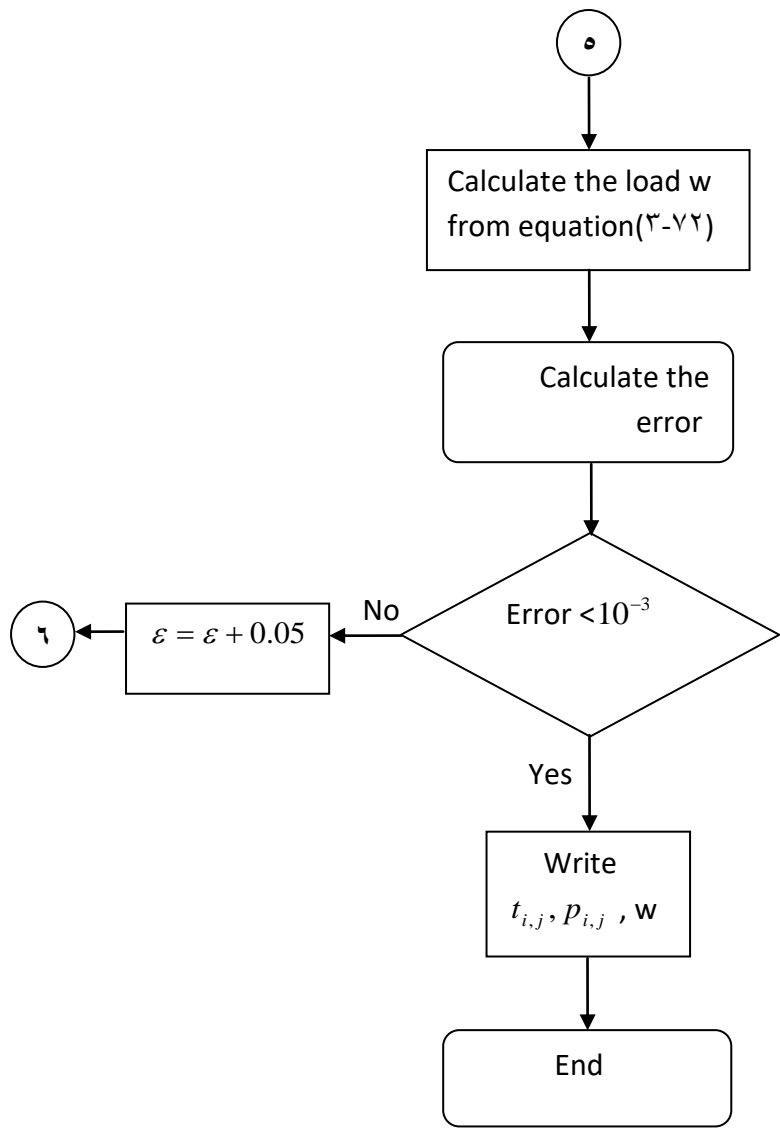


Fig.(3-5) Flowchart of Computer Program







RESULTIS AND DISCUSSION

Numerical results of a steady state performance for a finite length journal bearing obtained during this work are investigated through this chapter. The bearing was considered to have a single groove located at the crown of the bearing, on the line parallel to the load direction. The proposed bearing operating characteristics are presented in table (ε-1).

The effect of different operation parameters and geometric factors, namely, rotational speed, applied load, type of lubricant, inlet oil temperature, ambient temperature, and bearing clearance on the thermal behavior of the full and partial journal bearing are discussed below.

ε-1

Verification of the proposed modal

The maximum oil film temperature and pressure are calculated for a bearing working under different loading conditions and constant journal rotation speed (ε-1000 rpm). The maximum oil film temperature and pressure are presented at the mid-plane of the bearing. The results obtained are compared to that result obtained by J.Ferron et al. [2] as shown in figures (ε-1) and (ε-2). The results are seem to be in a good agreement with. The maximum deviation was found to be

τ for the maximum oil film temperature and ρ in the case of maximum oil film pressure.

The results obtained in the present work are also compared to the numerical results obtained by Nassab et al. and the experimental results obtained by J.Ferron et al.[19] as shown in figures (4-3) and (4-4). It seems from these figures that the results are in a good agreement with. The above comparisons represent a good verification to the computer program prepared to solve the problem of this work.

The effect of journal speed on the maximum oil film temperature is presented in figure (4-5). It can be shown from this figure that the maximum temperature in the oil film is greatly affected by the rotational speed. This is attributed to the effect of rotational speed on the shearing phenomenon. The maximum oil film pressure was also found to be greatly enhanced by rotational speed of the journal due to increasing the hydrodynamic effects as shown in figure (4-6).

The effect of journal speed and the eccentricity ratio on the location of the maximum bearing metal temperature can be shown in figure (4-7). It can be shown that the location of the maximum bearing bush temperature (t_b) moves in the direction of journal rotation as the journal speed increases while it moves in the reverse direction with the increase of the eccentricity ratio for the same journal speed.

The effect of the lubricant type on thermal behavior of journal bearing at a certain journal speed (1000 rpm) and the eccentricity ratio (0.5) can be shown in figures (4-8), (4-9), and (4-10). Three types of lubricants are used in this case (No.1, No.2, and No.3). The oil viscosity coefficients (k_o, k_1, k_2) of No.1 and 2 are

calculated from the viscosity-temperature curve published in [8]. The specification of these lubricants are presented in table (4-2). The temperature distribution of the bearing bush surface and the oil film at the mid-plane of the bearing were increased as the lubricant viscosity increased as shown in figures (4-9), and (4-10). This is due to the increase in friction force with the increase of viscosity but it is not at the same degree because of the oil temperature rise and its effect on oil viscosity. The effect of the lubricant viscosity on the oil film pressure distribution at the mid-plane of the bearing can be shown in figure (4-11). It is clear that using more viscous oil lead to a higher oil film pressure and applied load since oil film pressure is a function of oil viscosity as shown from the Reynolds' equation. On the other hand, the effect of the lubricant viscosity, at the same applied load, on oil film pressure, oil film temperature, and bearing bush temperature can be presented in figures (4-12), (4-13), and (4-14). Using more viscous oil leads to greater viscous dissipation and temperature rise in the oil film and bearing metal. An increase in the minimum oil film thickness was also seen, this is due to the reduction in the eccentricity ratio (from 0.69 with lubricant No.1 to 0.59 with lubricant No.2). It can be concluded that the effect of the lubricant viscosity on the temperature rise of the oil film and metal bearing in this case when the bearing working at the same load is less than that when the bearing working at the same eccentricity. This is due to the cooling effect of the oil flow.

The effect of the inlet oil temperature on the distribution in the bearing bush and oil film at the mid-plane of the bearing are presented in figures (4-15) and (4-16). It can be seen from these figures that the oil film temperature and the bush metal temperature are increased as the inlet oil temperature increases. It can also be shown that as the inlet oil temperature changed from 30°C to 40°C the maximum bearing bush temperature was increased only by 1.7°C. This can be attributed to the decrease in oil viscosity which causes a reduction in the viscous dissipation in this case.

The effect of the clearance on the thermal behavior of the journal bearing is presented in the figures (ε-16), and (ε-17). These figures show that the increase of bearing clearance leads to increase in the eccentricity ratio, decrease in the minimum oil film thickness (h_{min}) which causes the maximum oil film pressure at the mid-plane to be higher as shown in figure (ε-16). The increase of the bearing clearance causes an increase in the axial flow rate, and due to the low velocity gradient across the oil film, all the bearing temperatures decrease as can be observed for bush metal temperature in figure (ε-17).

Thermohydrodynamic behavior of a partial journal bearing with hollow shaft, in condition pertinent to that used in supporting the two necks of cement ball mills was also studied. The main data related to this bearing are presented in table (ε-2). The effect of the temperature of the hollow shaft which receives the heat from the ball mill body and the hot fluid passing through on the performance of the journal bearing coupled with the other operating parameters were studied as bellow:

The inner temperature of the hollow shaft (t_{si}) was appended to cover the effect of the two sources of heat(process effect) on the shaft temperature.

The effect of the inner temperature of the hallow shaft (t_{si}) on the behavior of the bearing can be shown in figures (ε-18), (ε-19), and (ε-20).

For the same applied load and journal rotational speed, when the shaft temperature(t_{si}) increases the maximum oil film pressure increases as a result of increasing the oil film temperature causing an increase in eccentricity ratio and hence, reduced minimum oil film thickness (h_{min}) as shown in figure (ε-19). More clear insight into the effect of the inner temperature of the hallow shaft on the temperature distribution in the bearing bush and the oil film can be gained by examining figures (ε-20) and (ε-21). It can be shown that when the shaft inner

temperature was changed from 30°C to 40°C the maximum bearing bush temperature was increased by 1.1°C suggesting that the higher temperature of the shaft causes higher conducted heat to the oil film and the bearing bush metal.

The effect of the inlet oil temperature on the temperature distribution in bearing bush metal can be shown in figures (4-21), (4-22), (4-23), and (4-24). Figure (4-21) shows the influence of the inlet oil temperature on the circumferential temperature distribution in bearing bush metal at the mid-plane of the bearing neglecting the effect of the hollow shaft as a heat source. It can be shown from these figures that when the inlet oil temperature increased by 10°C (from 30 to 40°C) the maximum bearing bush temperature increased only by 1.9°C due to reduction in viscous dissipation in oil film with the decrease in the oil viscosity.

Figures (4-22), (4-23), and (4-24) show the combined effect of the inlet oil temperature and the inner temperature of the hollow shaft on temperature distribution in the bearing bush metal and oil film. It can be shown from these figures that the increase of the inlet oil temperature causes a remarked effect on the temperature distribution in the first half of the bearing bush metal. At the inlet zone, the temperature of the bearing bush was effected by the inlet oil temperature and the bearing surrounding temperature (in this case 40°C) the effect of surrounding temperature becomes negligible at the second half of the bearing which is clear that as a small difference in the temperature distribution.

The effect of bearing surrounding temperature on the temperature distribution at the mid-plane of the bearing of partial journal bearing bush and oil film can be shown in figures (4-25) and (4-26). As shown in figure (4-25) when the bearing surrounding temperature increases by 10°C (from 30 to 40°C) the maximum bearing bush temperature increased by 1.6°C . This can be attributed to the effect of the surrounding temperature on the heat lost from the

bush surface. When the inner temperature of the hallow shaft reaches $60^{\circ}C$ as shown in figure (ε-26) with the same surrounding temperature the maximum bearing bush temperature at the mid-plane increased by $2.5^{\circ}C$ as shown in figure (ε-26).

The effect of lubricant type on the behavior of the partial journal bearing at the same applied load and journal rotational speed can be shown in figures (ε-27), (ε-28), (ε-29) and (ε-30). Two types of lubricant were used in this case (No.1) and (No.2). The oil viscosity coefficients (k_o, k_1, k_2) are calculated from the viscosity-temperature table of the Midland Refineries company-Iraq as presented in table (ε-ε). Figures (ε-27) and (ε-28) show the influence of lubricant type on circumferential temperature distribution in bearing bush metal and oil film pressure at the mid-plane of the bearing neglecting hallow shaft temperature. The effect of the lubricant viscosity on the oil film pressure distribution can be shown in figure (ε-29). The more viscous oil at the same applied load leads to increase minimum oil film thickness, decrease maximum oil film pressure, and increase maximum temperature in the bush metal at the mid-plane. Maximum bush metal temperature in this case was increased by $2^{\circ}C$ as shown in figure (ε-28). In other case as the effect of inner temperature of the hallow shaft is taken into consideration a small increase in maximum bush temperature is noticed and there is shifting in the temperature distribution curve. This can be attributed to the effect of larger oil film thickness when using more viscous oil as shown in figure (ε-30).

The effect of the bearing clearance on the behavior of the journal bearing is presented in the figures (ε-31), and (ε-32). Suggesting that for the high applied load ($50000N$ in this case) a decrease in minimum oil film thickness for higher bearing clearance in order to obtain an equilibrium in applied load as shown in figure(ε-31). The decrease in minimum oil film thickness in this case can also be seen as an increase in oil film temperature as shown in figure (ε-32).

Table(4-1): bearing characteristics used in test cases as reported by [6].

Parameter	Symbol	Unit	Value
Journal radius	R	m	0.05
External bearing radius	r_{bout}	m	0.1
Bearing length	L	m	0.08
Radial clearance	c	m	0.000150
Lubrication viscosity at ξ , $^{\circ}C$	μ	pa . s	0.0277
Viscosity coefficients	k_0		3.287
	k_1		3.64
	k_2		0.777
Lubrication density at ξ , $^{\circ}C$	ρ	kg/m ³	870
Lubrication specific heat	C_o	J/kg. $^{\circ}C$	2000
Lubrication thermal conductivity	k_{oil}	W/m. $^{\circ}C$	0.13
Bush thermal conductivity	k_b	W/m. $^{\circ}C$	200
Shaft thermal conductivity	k_s	W/m. $^{\circ}C$	50
Convection heat transfer coefficient	h_{conv}	W/m ² . $^{\circ}C$	80
Inlet oil temperature	t_{in}	$^{\circ}C$	40
Ambient temperature	t_a	$^{\circ}C$	40
Inlet lubricant pressure	p_s	Pa	180000
Groove angle		deg	18

Table(4-2): Partial bearing characteristics used in test case.

Parameter	Symbol	Unit	Value
Journal radius	R	m	0.9
External bearing radius	r_{bout}	m	0.972
Bearing length	L	m	0.9
Radial clearance	c	m	0.0017
Lubrication viscosity at $\xi, ^\circ C$	μ	pa . s	0.241
Viscosity coefficients	k_0		3.7714
	k_1		3.0827
	k_2		0.9112
Lubrication density at $\xi, ^\circ C$	ρ	kg/m ³	870
Lubrication specific heat	C_o	J/kg. $^\circ C$	2000
Lubrication thermal conductivity	k_{oil}	W/m. $^\circ C$	0.13
Bush thermal conductivity	k_b	W/m. $^\circ C$	0.
Shaft thermal conductivity	k_s	W/m. $^\circ C$	0.
Convection heat transfer coefficient	h_{conv}	W/m ² . $^\circ C$	8.
Inlet oil temperature	t_{in}		40
Ambient temperature	t_a	$^\circ C$	40
Inlet lubricant pressure	p_s	$^\circ C$	0.
Bearing arc e		Pa deg	120.

Parameter	No.1 ISO VG ٢٢ # ٩٠ Turbine oil	No.٢ ISO VG ٣٢	No.٣ #١٤٠ Turbine oil
-----------	------------------------------------	-------------------	--------------------------

Table(٤-٣) Lubricants specification*.

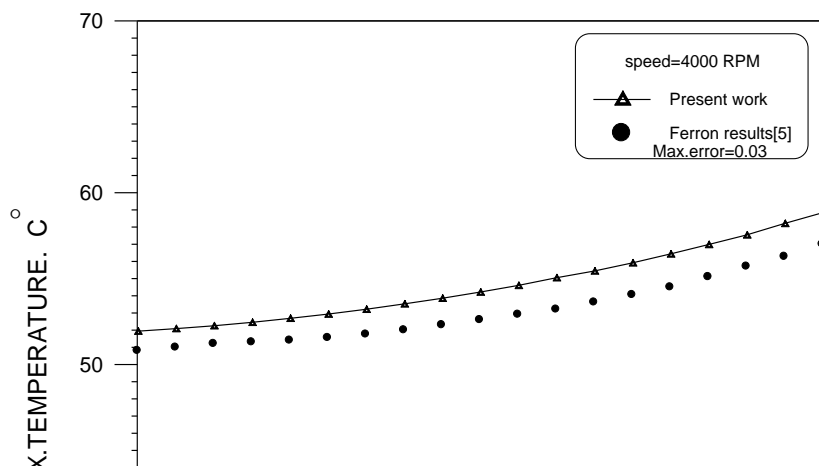
* The lubricants specification were reported by [٨].

Lubrication viscosity at $\xi \cdot ^\circ C$	0.192 pa. s	0.277 pa. s	0.469 pa. s
Viscosity coefficients			
k_0	4.10039	3.287	4.38776
k_1	4.23349	3.064	4.70906
k_2	1.1329	0.777	1.3218

Table (4-4) Lubricants specification*.

Parameter	No.1 ISO VG 100 Code: 04.1	No. ISO VG 220 Code: 04.2
Lubrication viscosity at $\xi \cdot ^\circ C$	0.12 pa. s	0.241 pa. s
Viscosity coefficients		
k_0	3.6714	3.6714
k_1	3.0826	3.0826
k_2	0.9112	0.9112

* The lubricants specification were reported by the Midland Refineries company-Iraq.



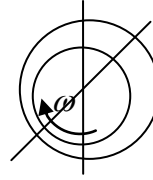


Fig.(4-1) The maximum oil film temperature versus eccentricity ratio

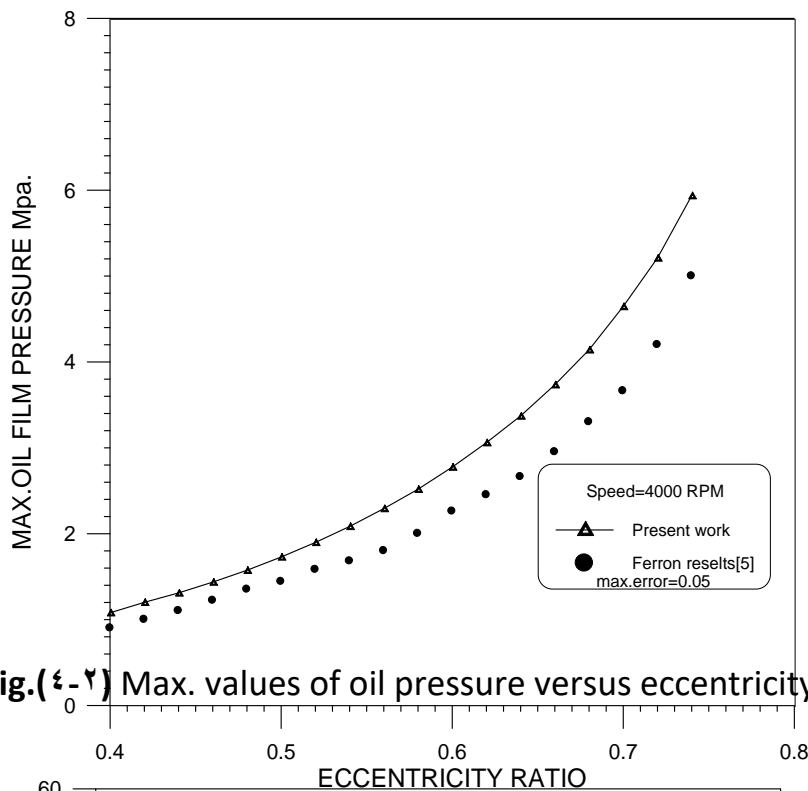


Fig.(4-2) Max. values of oil pressure versus eccentricity ratio

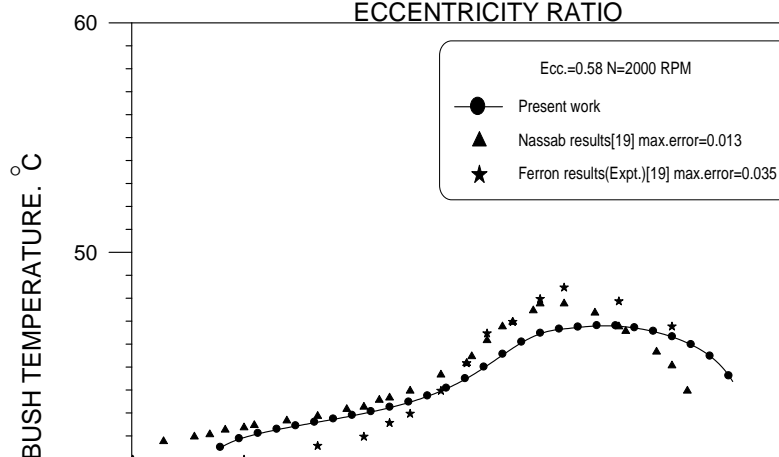




Fig.(٤-٣) Temperature distribution for Ferron[°] bearing bush

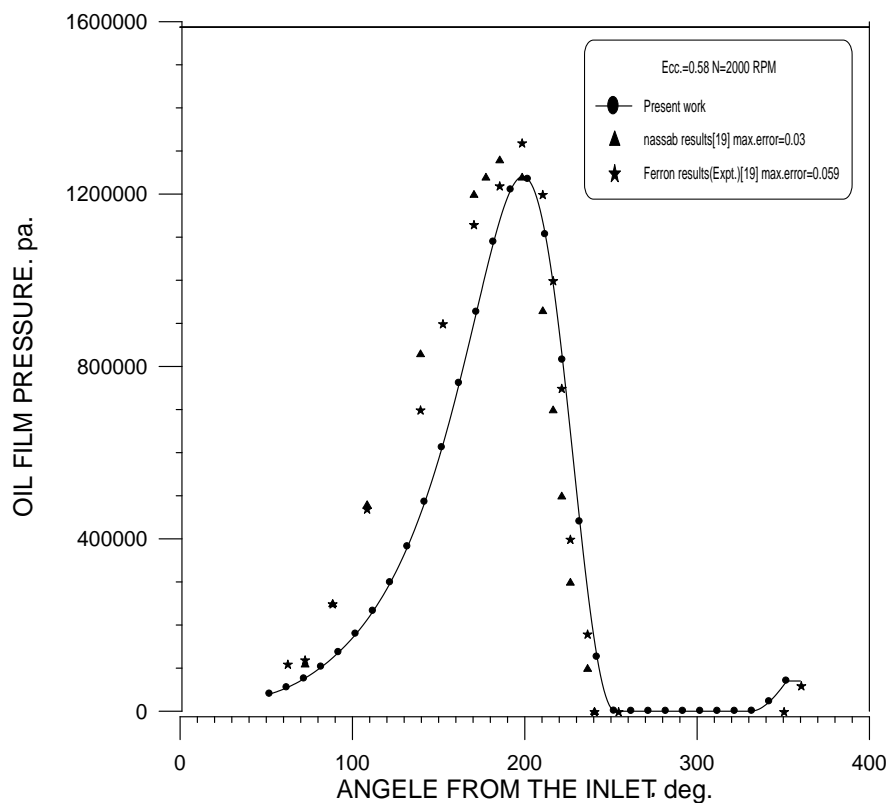


Fig.(٤-٤) Oil film pressure distribution for Ferron bearing

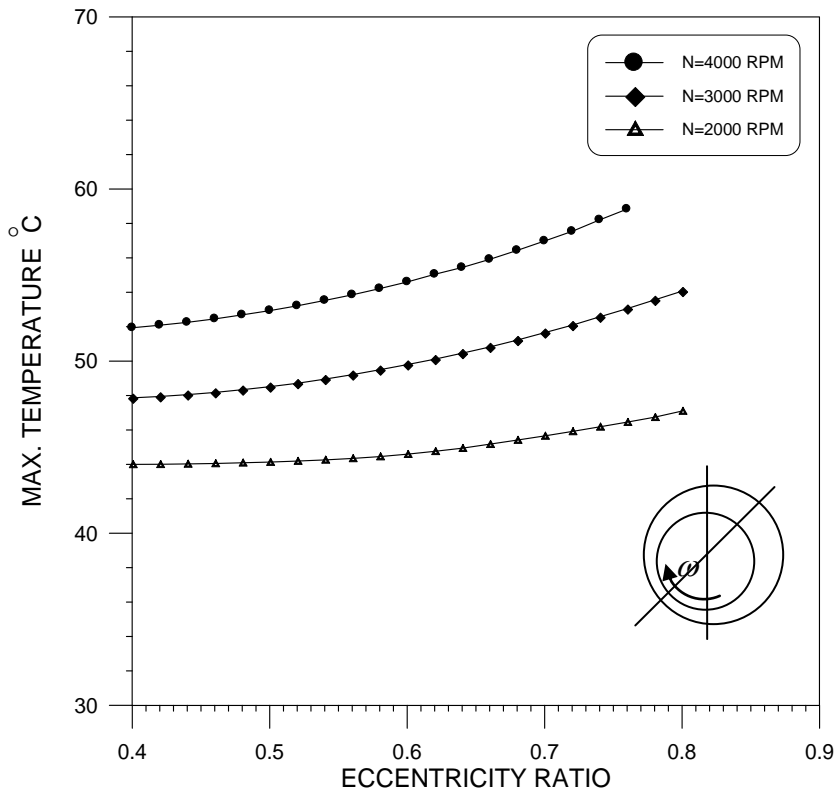


Fig.(4-5) Maximum values of temperature versus eccentricity ratio for different speeds

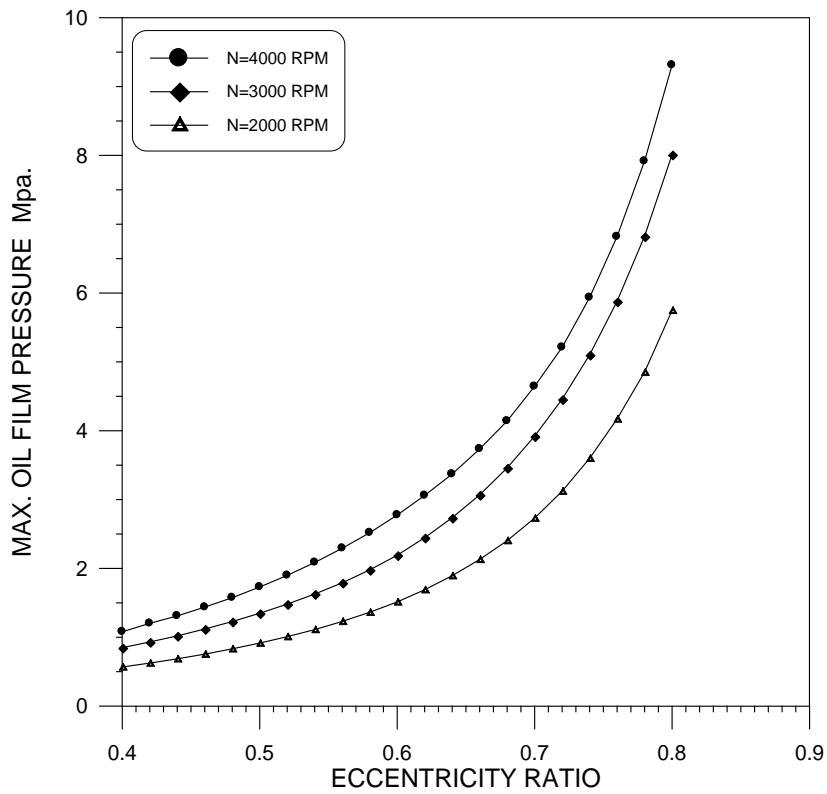


Fig.(4-6) Maximum values of oil pressure versus eccentricity ratio for different speeds

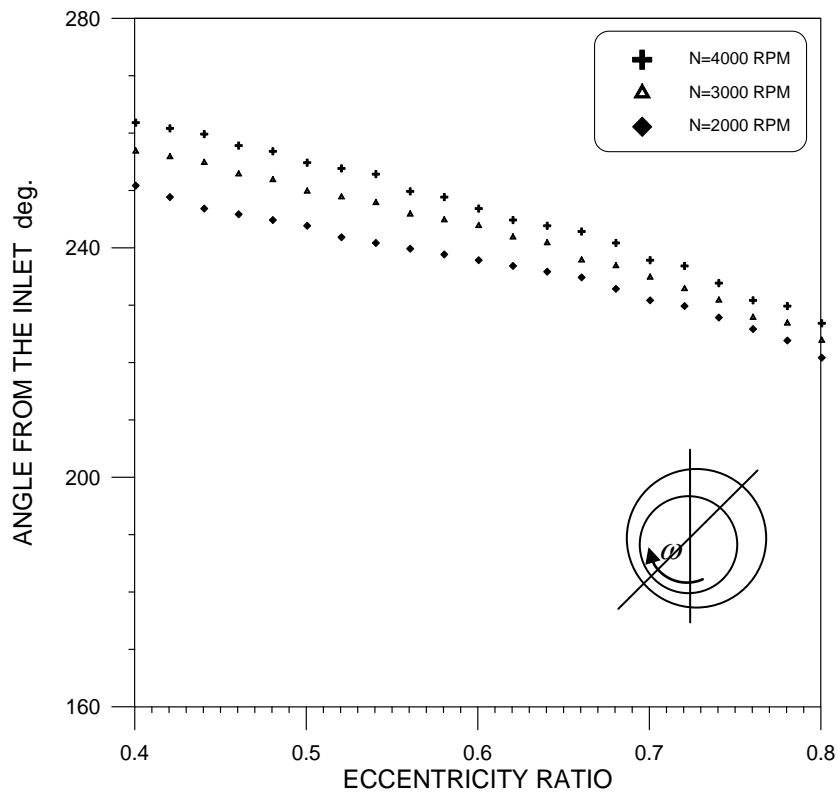


Fig.(4-V) Location of maximum bearing metal temperature

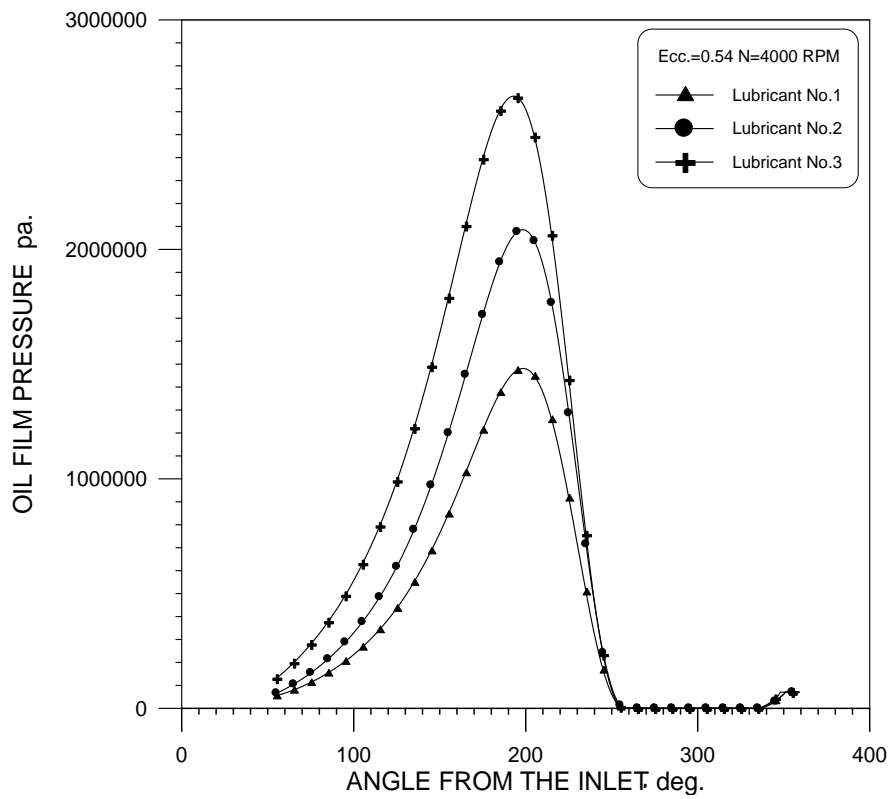


Fig.(4-Λ) Effect of lubricant viscosity on the oil film pressure distribution

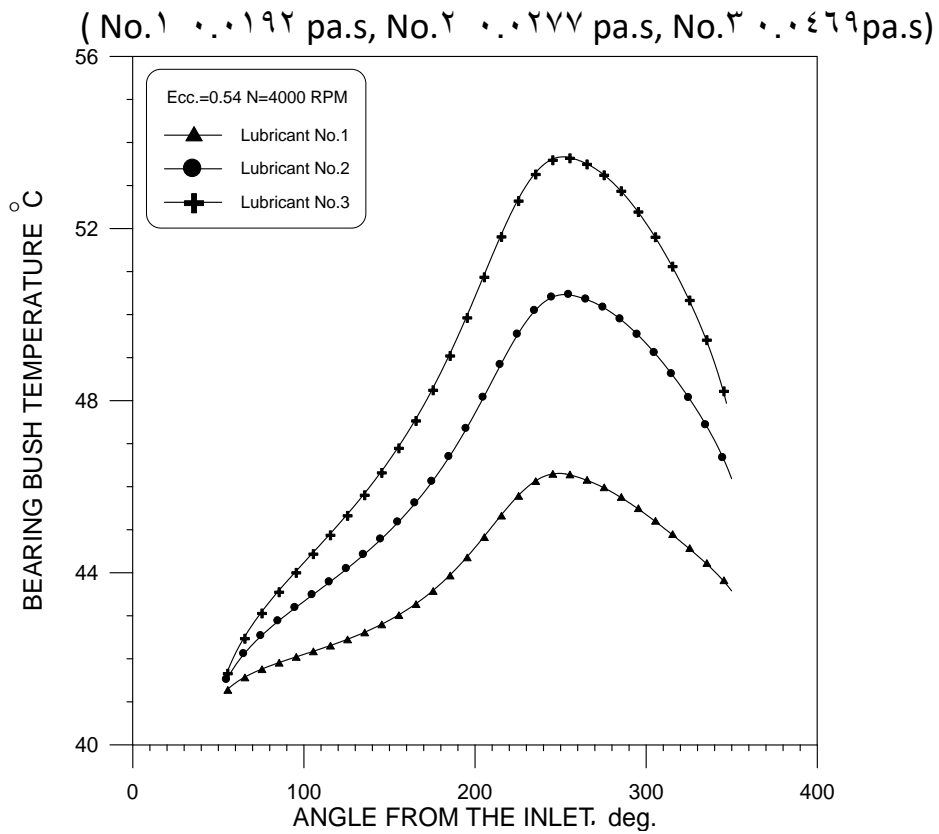


Fig.(4-9) Effect of lubricant viscosity on the temperature distribution of the bearing bush

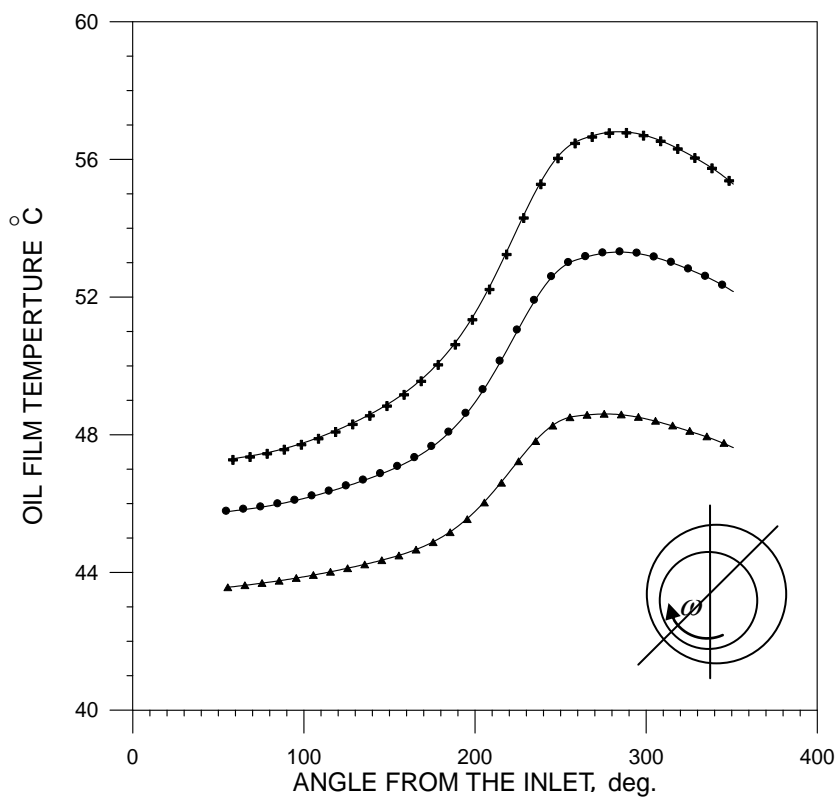


Fig.(4-10) Effect of lubricant viscosity on the temperature

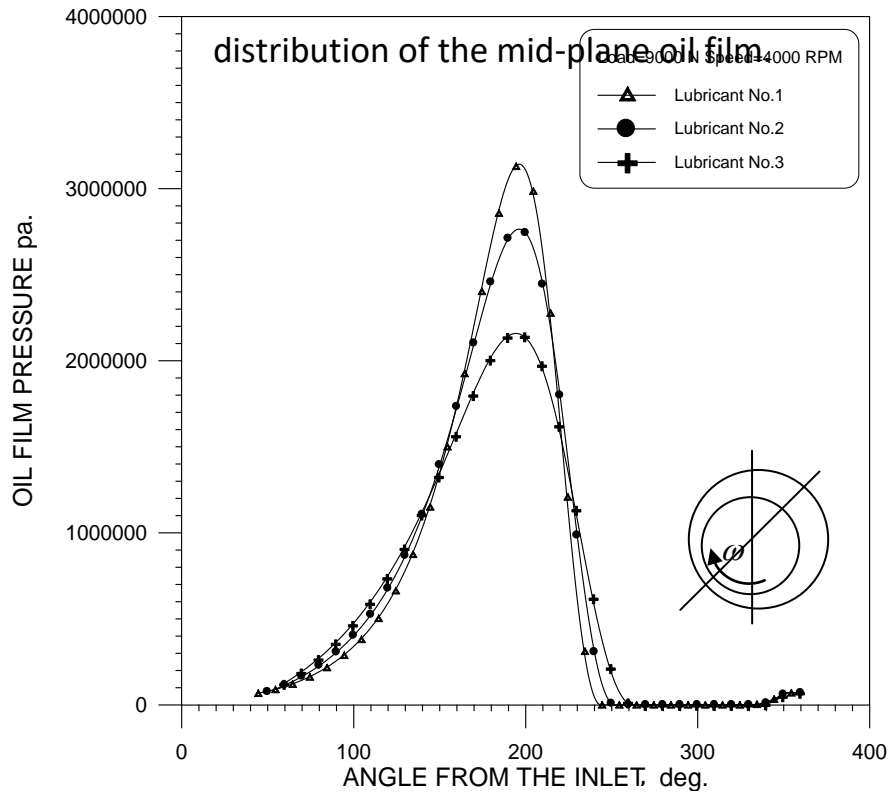


Fig.(4-11) Effect of lubricant viscosity on the oil film pressure

distribution with same applied load

(No.1) 0.192 pa.s, No.2) 0.277 pa.s, No.3) 0.469 pa.s)

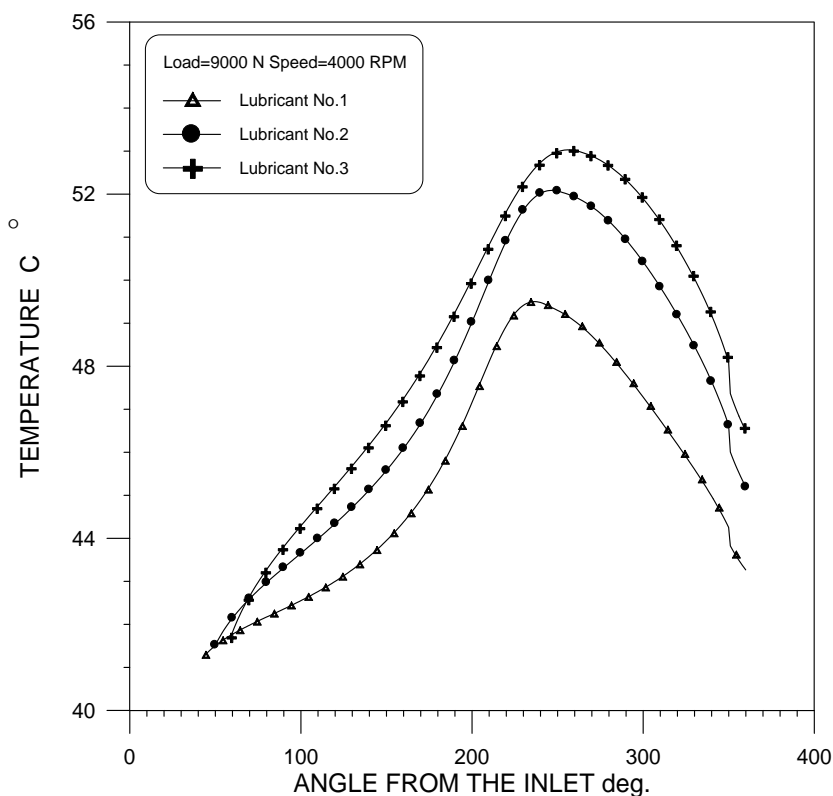


Fig.(٤-١٢) Effect of lubricant viscosity on the temperature distribution of the bearing bush with same applied load

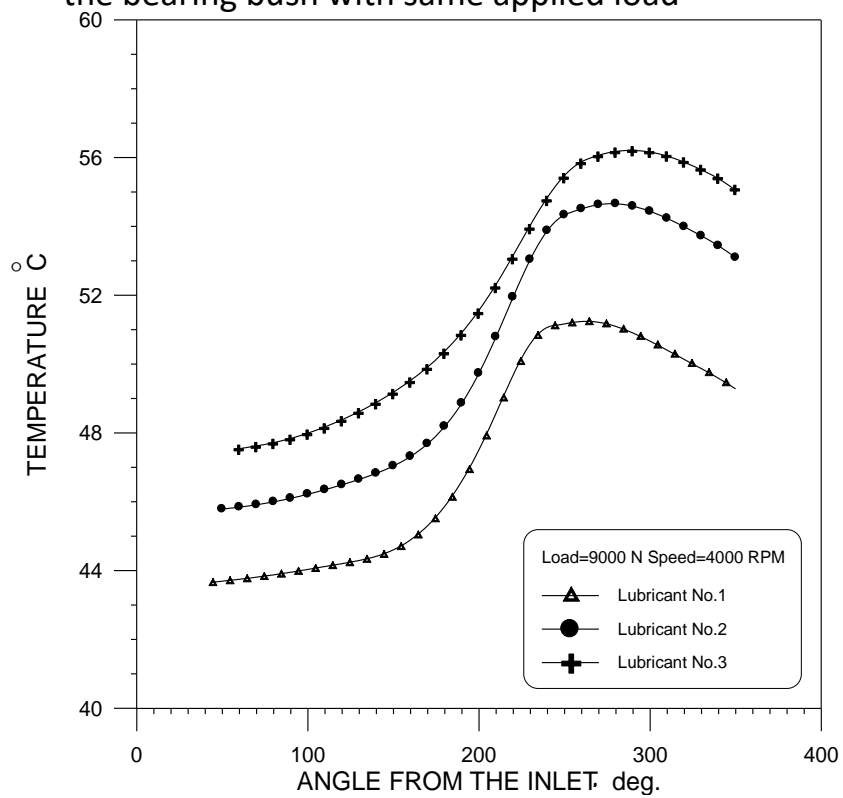


Fig.(٤-١٣) Effect of lubricant viscosity on the temperature distribution on the med-plane of the oil film with same applied load

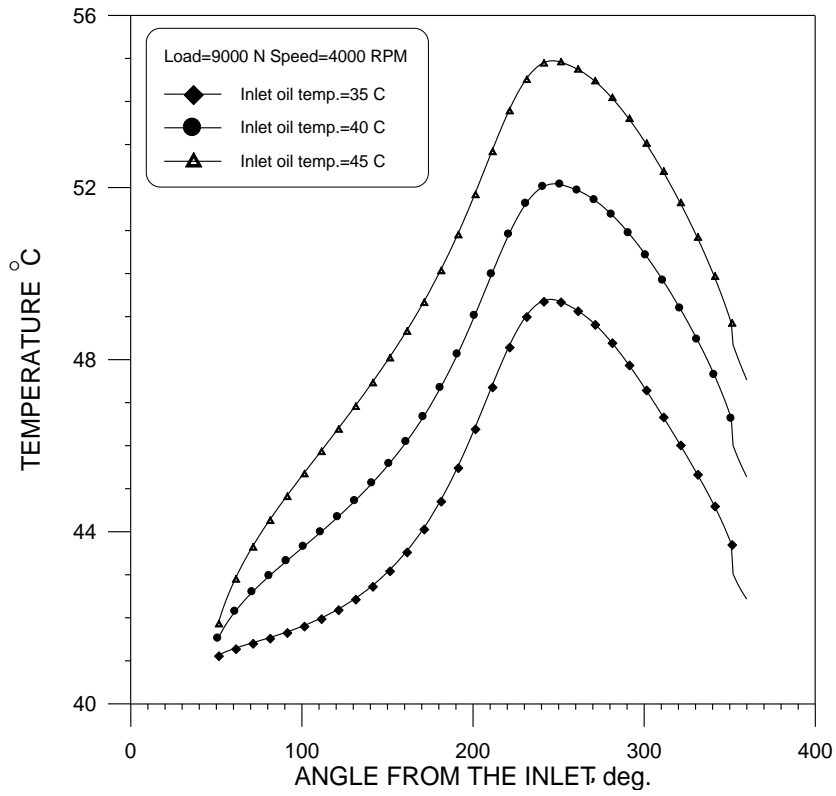


Fig.(4-14) Effect of the inlet oil temperature on the temperature distribution of the bearing bush

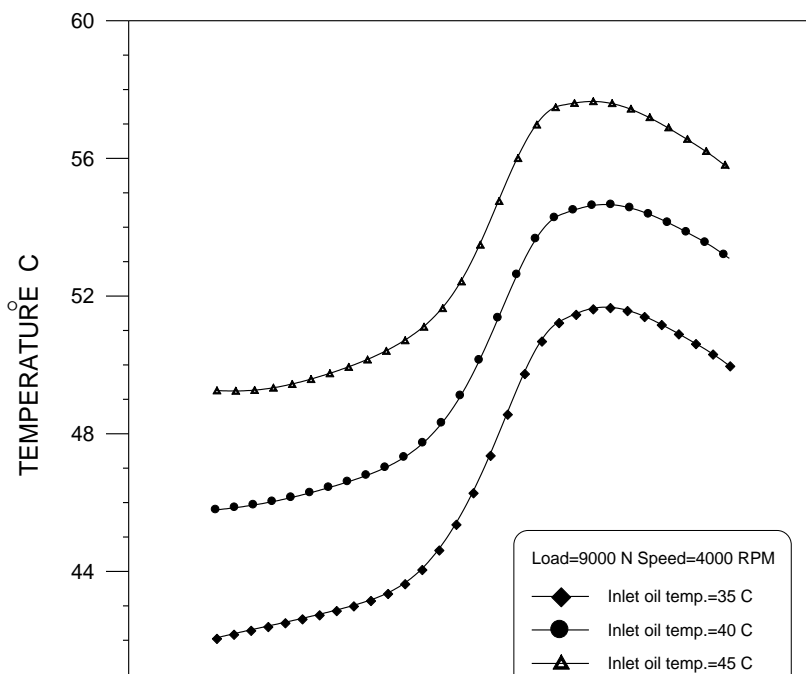


Fig.(4-15) Effect of inlet oil temperature on the oil film temperature distribution

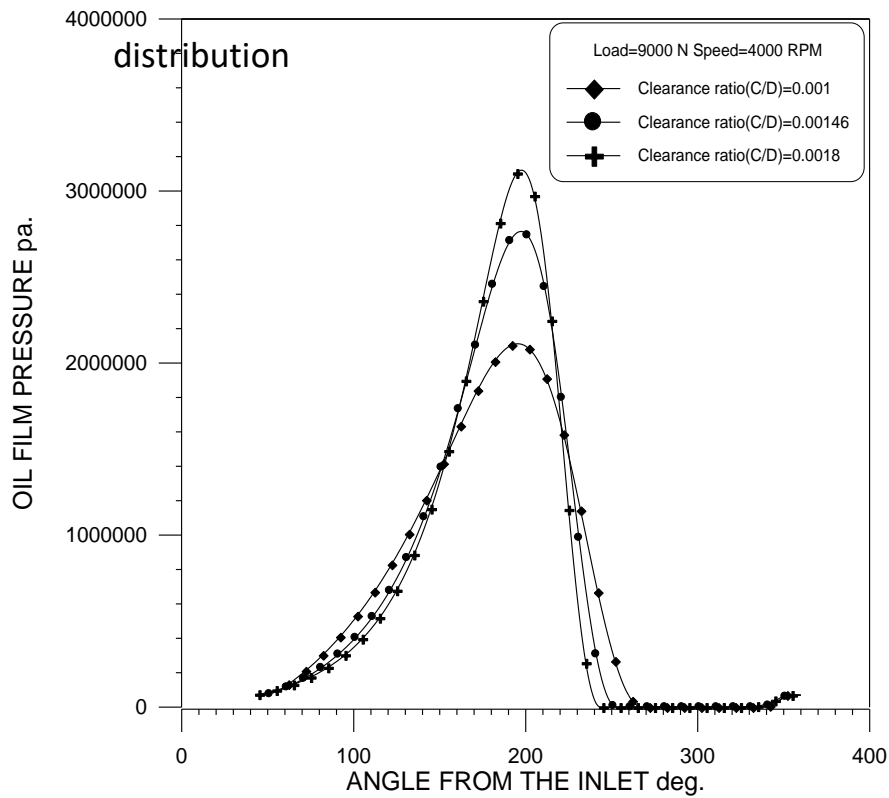


Fig.(4-16) Effect of clearance ratio on the oil film pressure distribution

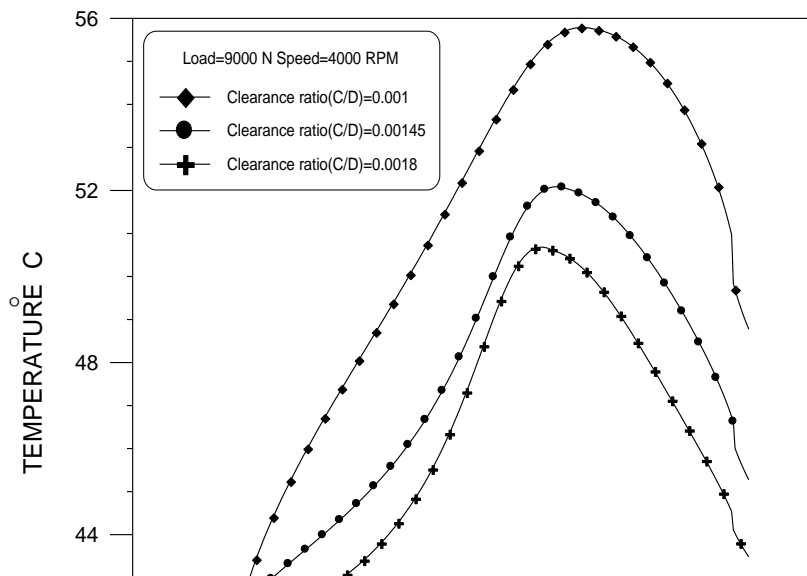


Fig.(4-17) Effect of clearance ratio on the temperature distribution of the bearing bush

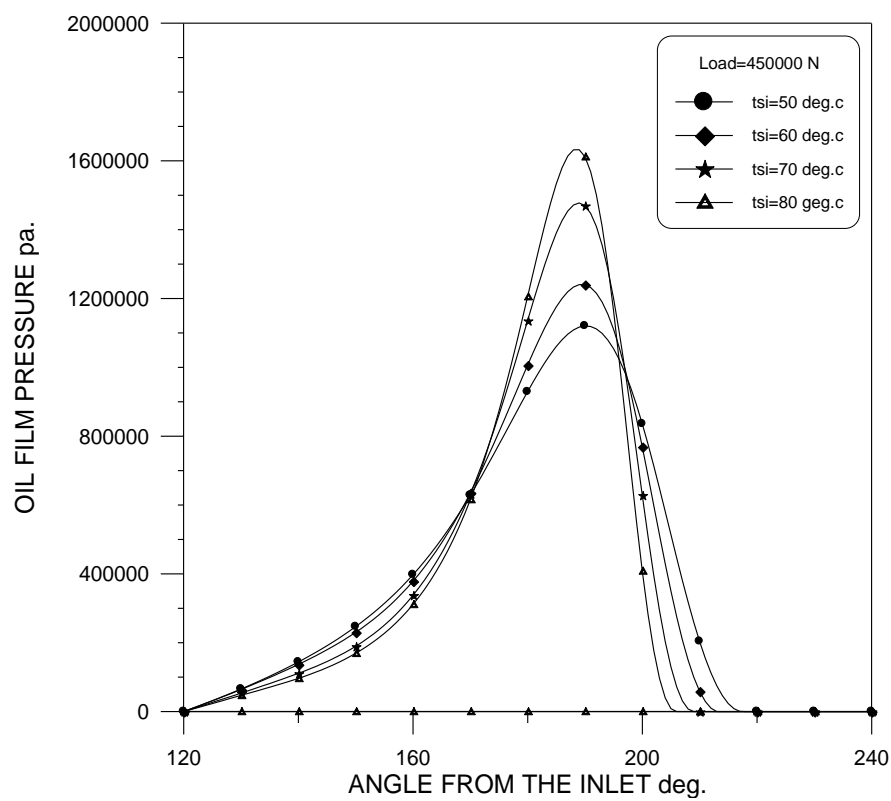


Fig.(4-18) Effect of inner temperature of the hollow shaft on the oil film pressure distribution for a partial journal bearing

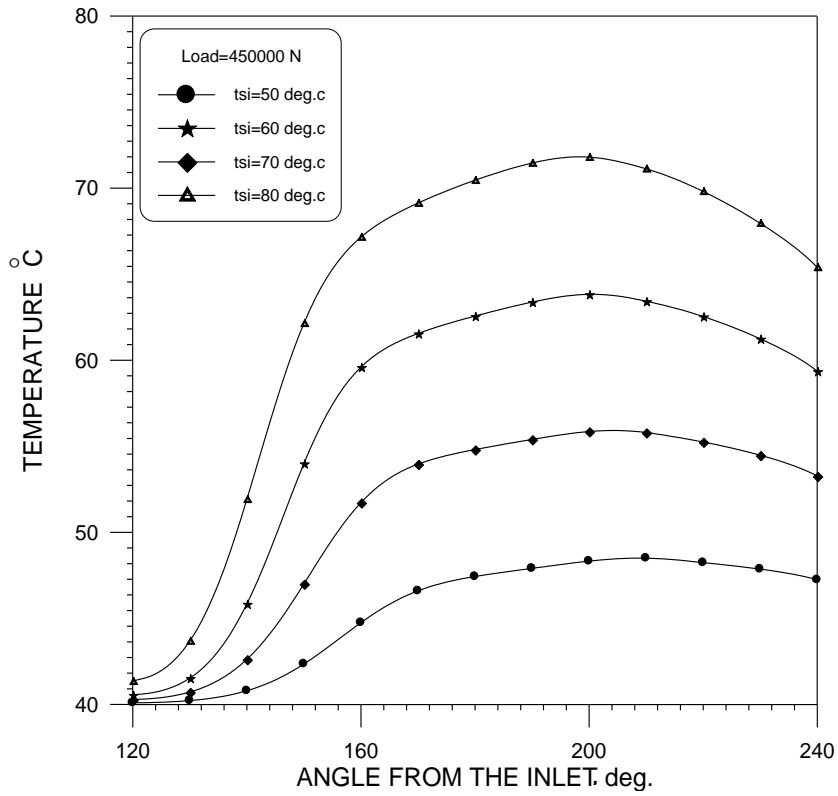


Fig.(4-19) Effect of inner temperature of the hollow shaft on temperature distribution of a partial journal bearing bush

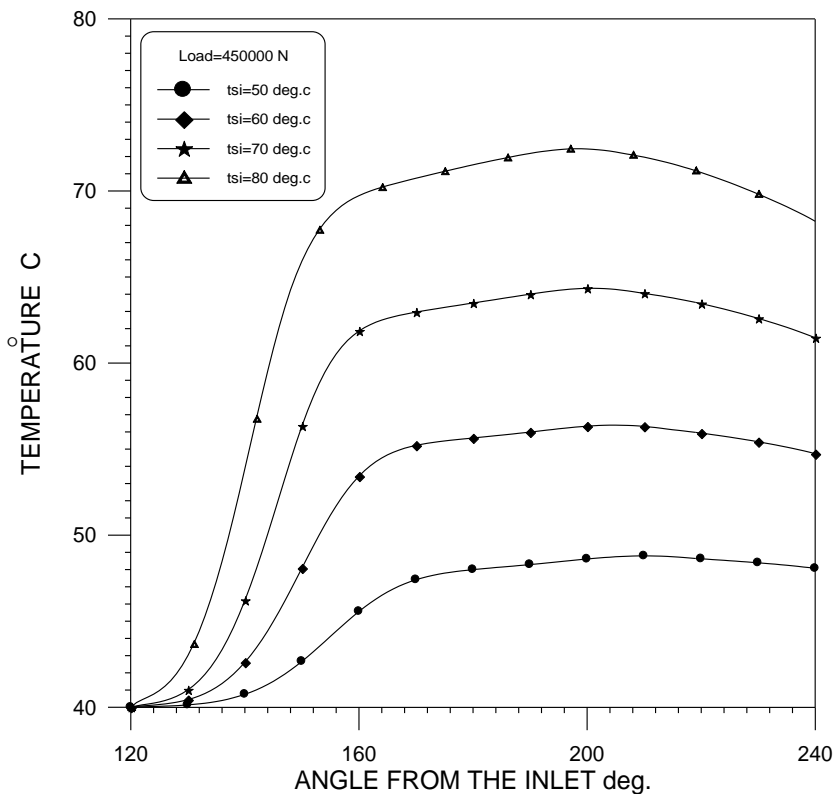


Fig.(4-20) Effect of inner temperature of the hollow shaft on the oil film temperature distribution a partial journal bearing

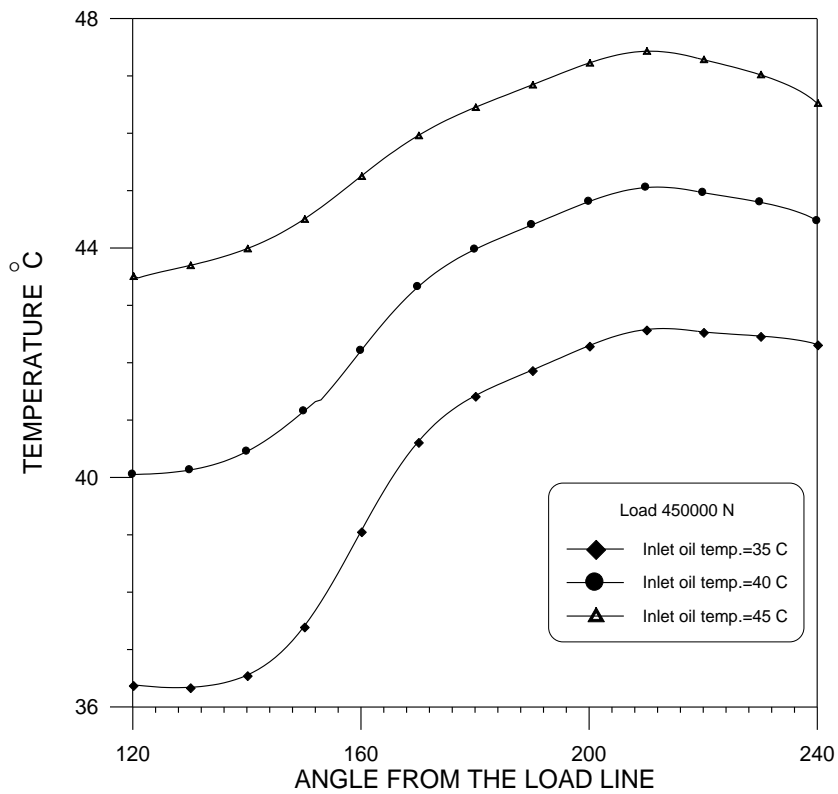


Fig.(4-21) Effect of inlet oil temperature on the temperature distribution of the partial bearing bush without effect of inner temperature of the hollow shaft

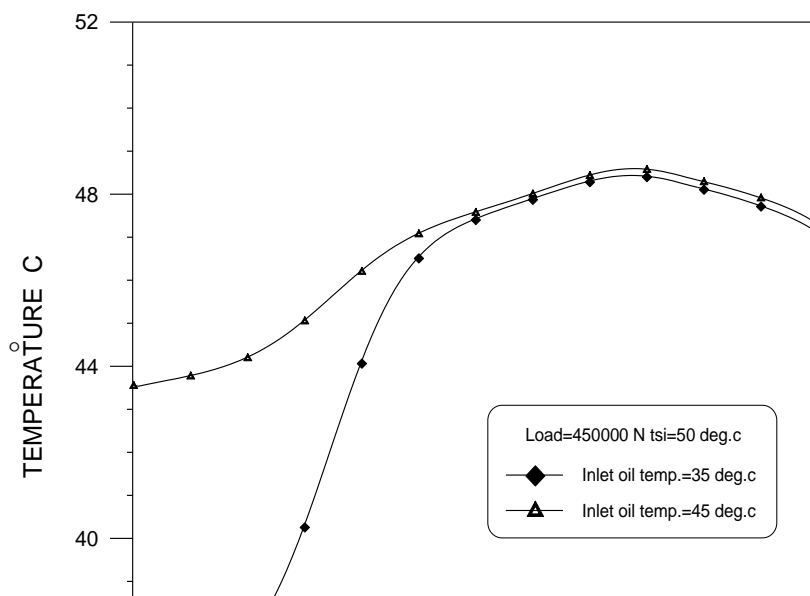


Fig.(٤-٢٢) Effect of inlet oil temperature on the temperature distribution of the partial bearing bush ($t_{si}=0 \text{ } ^\circ\text{C}$)

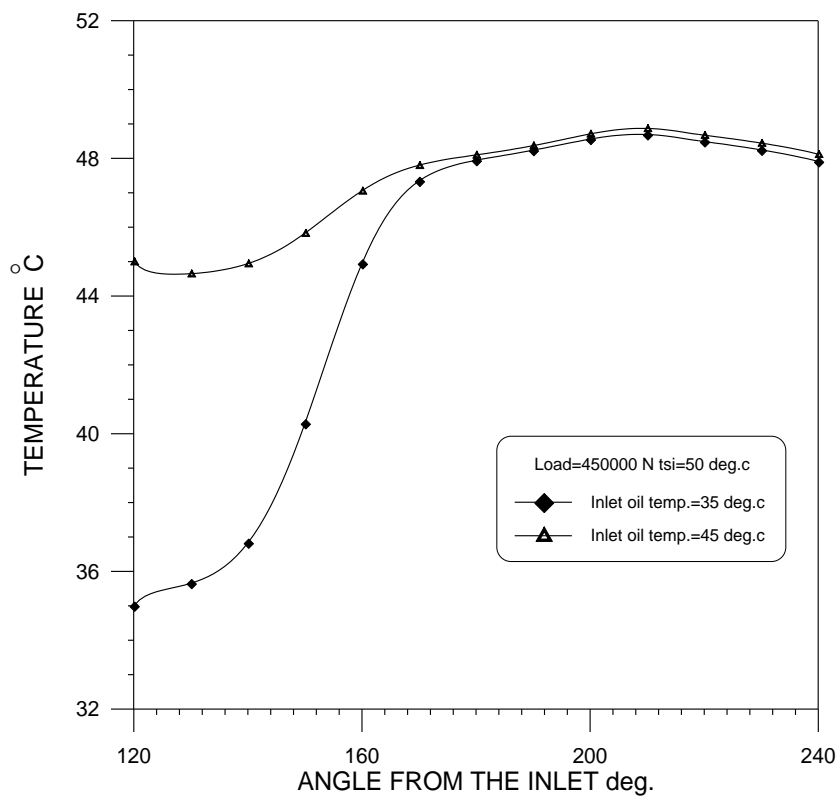


Fig.(٤-٢٣) Effect of inlet oil temperature on the oil film temperature distribution of a partial bearing ($t_{si}=0 \text{ } ^\circ\text{C}$)

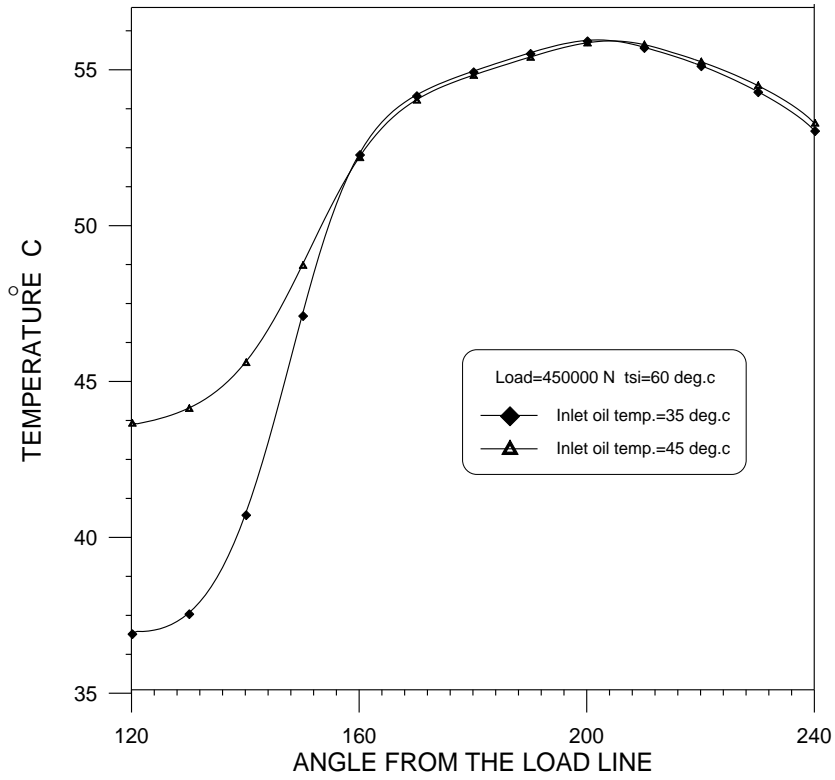


Fig.(4-24) Effect of inlet oil temperature on the temperature distribution of the partial bearing bush ($t_{si}=60\text{ }^{\circ}\text{C}$)

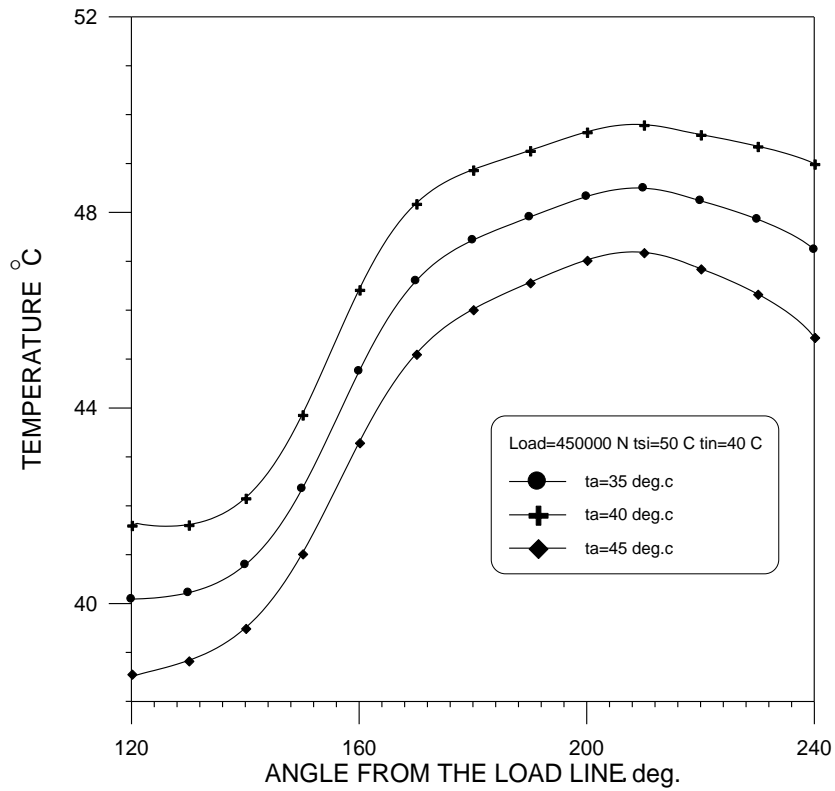


Fig.(4-25) Effect of ambient temperature on the temperature distribution

of partial bearing bush($t_{si}=0 \cdot ^\circ C$)

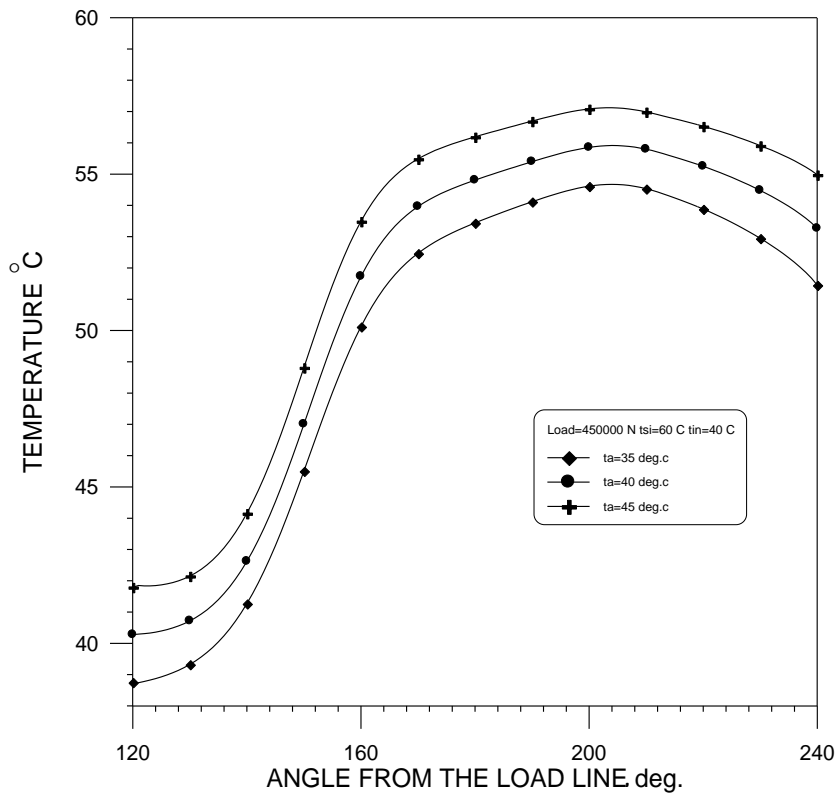


Fig.(4-26) Effect of ambient temperature on the temperature distribution

of partial bearing bush($t_{si}=6 \cdot ^\circ C$)

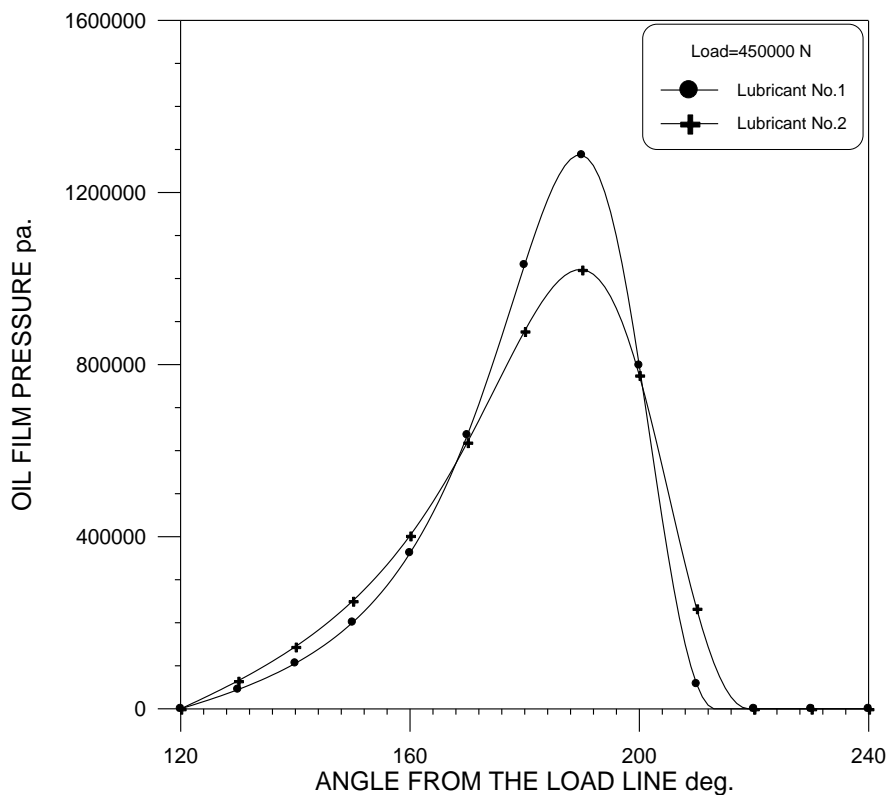


Fig.(4-27) Effect of lubricant viscosity on the oil film pressure distribution of a partial bearing with out effect of inner temperature of the hollow shaft

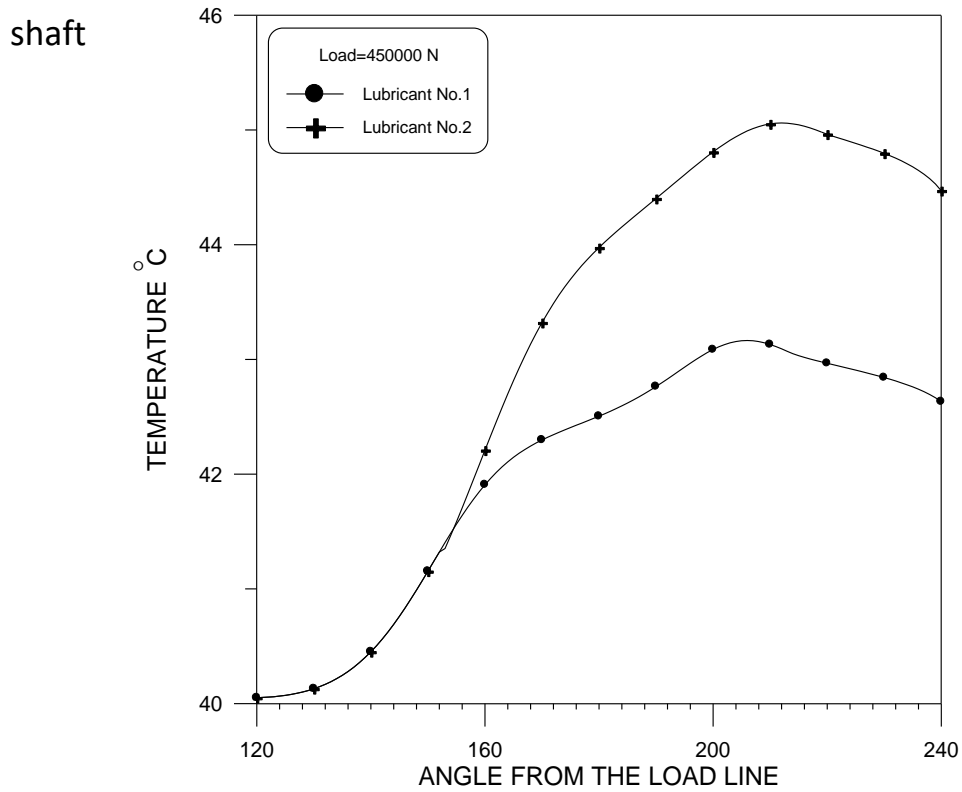


Fig.(4-28) Effect of lubricant viscosity on the temperature distribution of the partial bearing bush with out effect of inner temperature of the hollow shaft

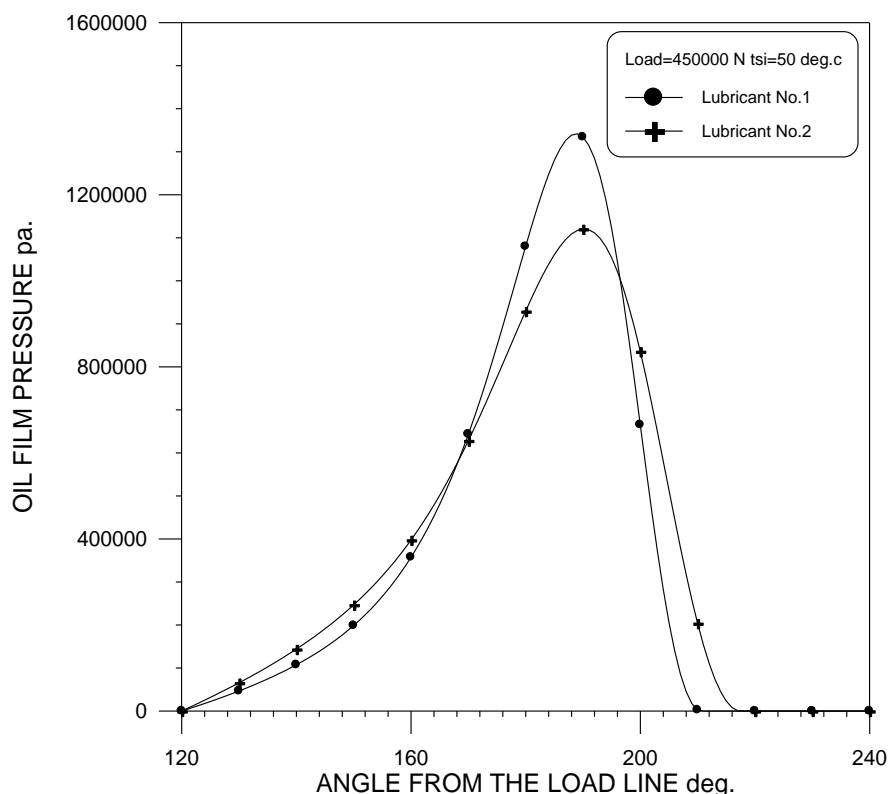


Fig.(4-29) Effect of lubricant viscosity on the oil film pressure distribution of

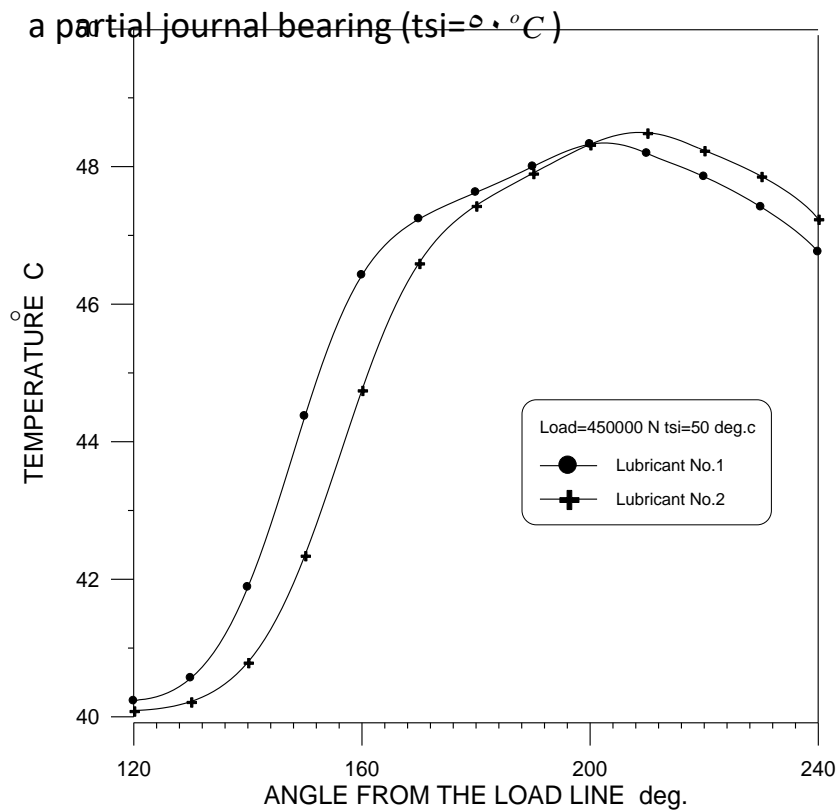


Fig.(4-30) Effect of lubricant viscosity on the temperature distribution of a

partial journal bearing bush ($t_{si} = 50, ^\circ C$)

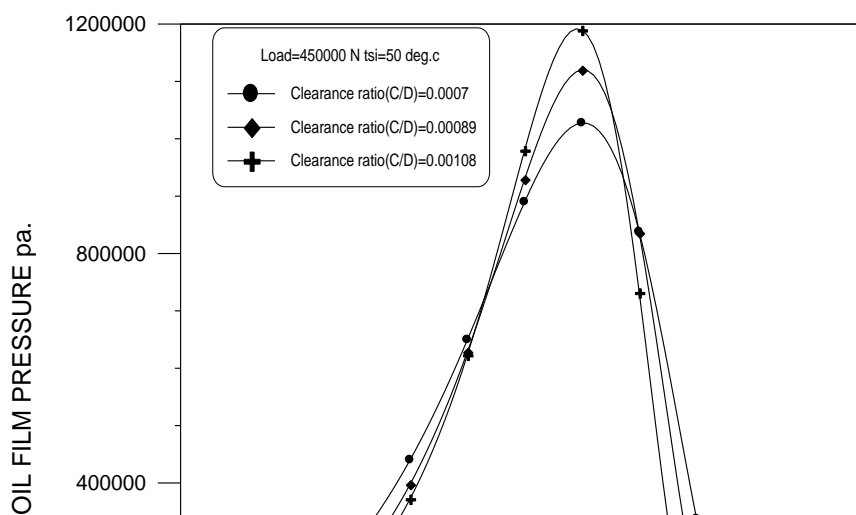


Fig.(4-31) Effect of clearance ratio on the oil film pressure distribution of a

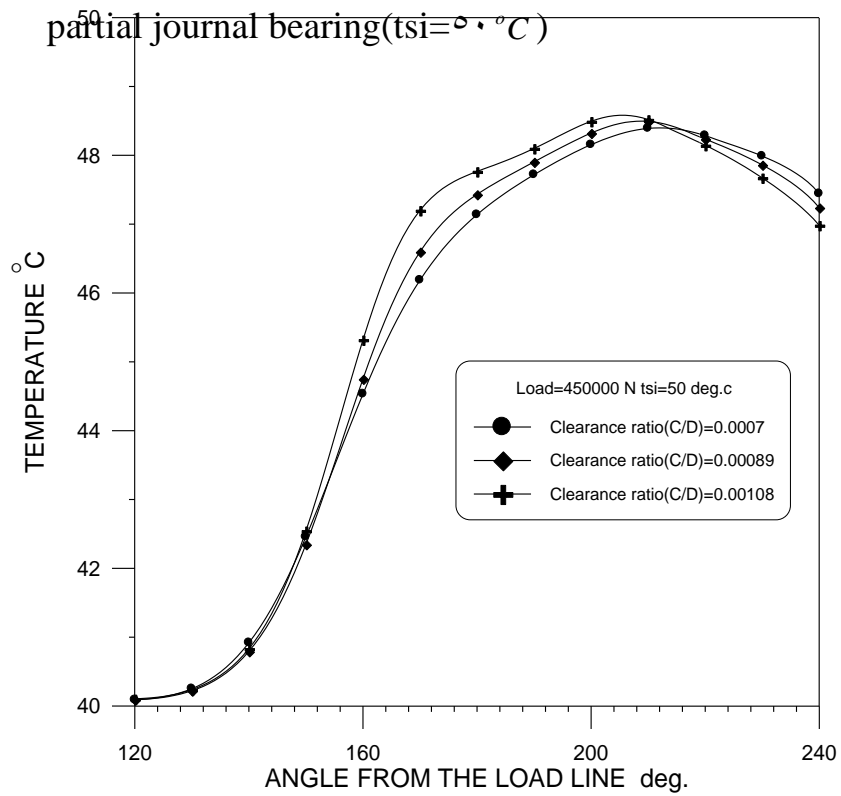
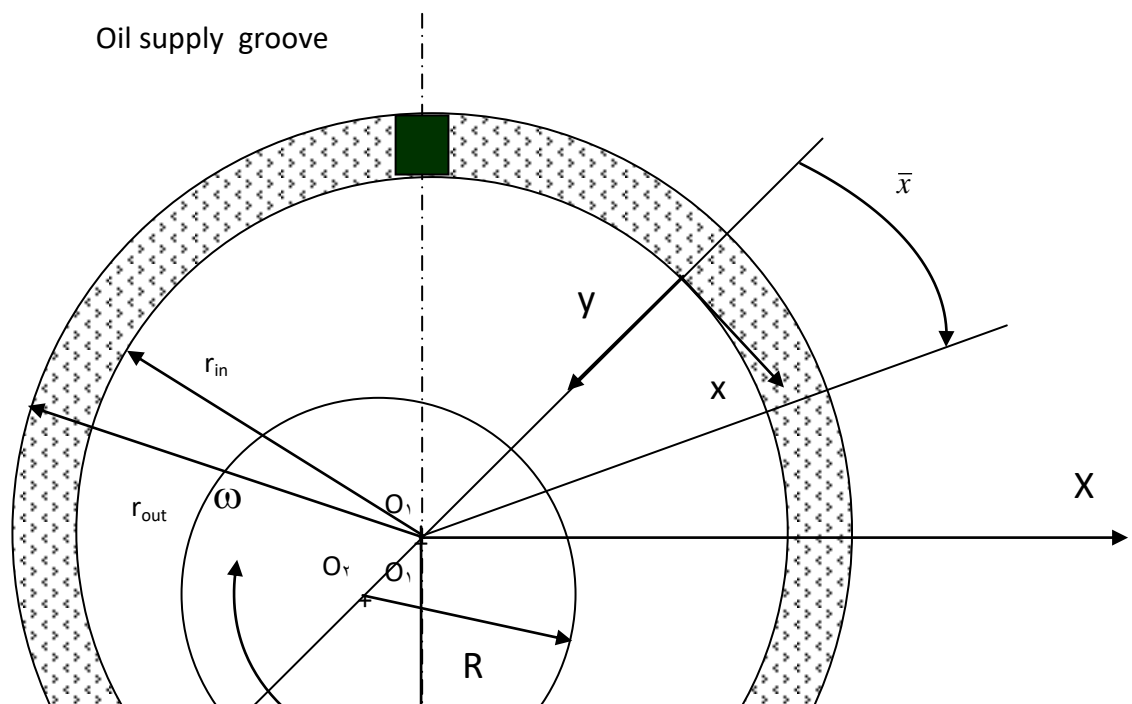


Fig.(4-32) Effect of clearance ratio on the temperature distribution of a partial journal bearing bush($t_{si} = 0^\circ C$)



CONCLUSIONS AND SUGGESTIONS FOR

FUTURE WORK

Thermohydrodynamic lubrication model for a finite length full and partial journal bearings have been implemented in this work. The primary

purpose of this thesis was to investigate the effect of different operational and geometrical parameters on the steady state operation of such bearings.

٥.١

Conclusions

The results obtained during this work leads to the following concluding remarks.

٥.١.١

Full journal bearing

- ١- The maximum oil film and bearing bush temperature at the mid-plane of the journal bearing increases with the increase of journal speed, lubricant viscosity, oil supply temperature and with the decrease of bearing clearance.
- ٢- The angular position of maximum bearing bush temperature moves in the direction of rotation as the journal speed increases, while contrary happens with the increase of eccentricity ratio.

٥.١.٢

Partial journal bearing

In the case of the partial journal bearing with hollow shaft and hot materials flow through it, the following concluding remark can be drawn:

- ١- The maximum oil film and bearing bush temperatures increases with the increase of the hollow shaft temperature.
- ٢- The maximum oil film pressure increases and the minimum oil film thickness decreases with the increase of the hollow shaft temperature.
- ٣- Due to the effect of the shaft temperature on the bearing, a small change in the maximum bearing bush temperature remarked with the change of supplied oil temperature, bearing surrounding temperature, clearance ratio, and lubricant viscosity.

It is clear that the effect of the temperature of the hollow shaft on the thermal behavior of the partial journal bearing in this case study is the dominant operation parameter. As remarked above the increase of the shaft temperature is led to an increase in the eccentricity ratio and, a reduce in the minimum oil film thickness which is limited the operation temperature of the journal bearing. To prevent metal-to-metal contact and increase the running times of cement mills, firstly the grinding process must be controlled to reduce the generative heat by increase the flow rate of air and water inside the mill body, increase the feeding rate of the mill, and reduce the temperature of the fed material, secondly the face of the hollow shaft of the bearing must be cooled by splashing oil on it.

The partial journal bearing is one of the most important type of supporting device in heavy machines. It needs expansion in the study of the performance of such bearings. Further work should be carried out, accounting for the following points:

- ϸ- An experimental study concerning the effect of operation parameters on the thermal behavior of the partial journal bearing.
- Ϲ- An experimental and a theoretical study concerning the effect of the partial arc length on dynamic performance and the thermal behavior of the partial journal bearing.
- Ϻ- A theoretical study concerning the dynamic performance and the thermal behavior of the partial journal bearing lubricated with Bi – phase (liquid – solid) lubricant.
- ϻ- A study of the chamfering effect on the thermal behavior and the dynamic performance journal bearing.

REFERENCES

1. **Oscar P., and Sargit S.**, "Adiabatic Solution for Finite Journal Bearing", Transaction of the ASME, vol. 101, pp. 492-496, October 1979.
2. **T. Suganami, and A. Z. Szeri**, "A Parametric Study of Journal Bearing Performance: The λ Partial Arc Bearing", Transaction of the ASME, vol. 101, pp. 486-491, October 1979.
3. **E. W. Cowking**, "Thermohydrodynamic Analysis of Multi-Arc Journal Bearing", TRIBOLOGY international, pp. 217-223, August 1981.
4. **A. Seieg, and S. Dandage**, "Empirical Design Procedure for the Thermohydrodynamic Behavior of Journal Bearings", Journal of Lubrication Technology, vol. 104, pp. 130-148, April 1982.
5. **J. Ferron, J. Frene, and R. Boncompain**, "A Study of the Thermohydrodynamic Performance of a Plain Journal Bearing Theory and Experiments", Transaction of the ASME, vol. 105, pp. 422-428, July 1983.
6. **J. Mitsui, Y. Hori, and M. Tanaka**, "Thermohydrodynamic Analysis of Cooling Effect of Supply Oil in Circular Journal Bearing", Transaction of the ASME, vol. 105, pp. 414-421, July 1983.
7. **J. W. Lund, and P. k. Hansen**, "An Approximate Analysis of the Temperature Conditions in a Journal Bearing. Part 1: Theory", Transaction of the ASME, vol. 106, pp. 228-106, April 1984.

8. **J. Mitsui, Y. Hori, and M. Tanaka**, "An Experimental Investigation on the Temperature Distribution in Circular Journal Bearings", *Journal of Tribology*, vol. 108, pp. 621-626, October 1986.
9. **R. Boncompain, M. Fillon, and J. Frene**, "Analysis of Thermal Effects in Hydrodynamic Bearings", *Journal of Tribology*, vol. 108, pp. 219-224, April 1986.
10. **H. Heshmat, and O. Pinkus**, "Mixing Inlet Temperatures in Hydrodynamic Bearings", *Journal of Tribology*, vol. 108, pp. 231-248, April 1986.
11. **J. Mitsui**, "A Study of Thermohydrodynamic Lubrication in A Circular Bearing", *TRIBOLOGY international*, vol. 20, pp. 331-441, December 1987.
12. **M. M. Khonsari, and V. Esfahanian**, "Thermohydrodynamic Analysis Solid-Liquid Lubricated Journal Bearing", *Journal of Tribology*, vol. 110, pp. 367-374, April 1988.
13. **M. M. Khonsari, and H. J. Kim**, "On Thermally Induced Seizure in Journal Bearings", *Journal of Tribology*, vol. 111, pp. 661-666, October 1989.
14. **Khonsari, M. M. Jang, J. Y., and Fillon**, "On the Generalization of Thermodynamic Analyses for Journal Bearings", *Journal of tribology*, vol. 118, pp. 517-519, 1996.
15. **Ma. M. and Taylor. C. M.**, "An Experimental Investigation of Thermal Effects in Circular and Elliptical Plan Journal Bearings", *Tribology International*, Vol. 29, pp. 19-26, 1996.

۱۶. **L. Costa, M. Fillon, A. S. Miranda, and J. C. P. Claro**, "An Experimental Investigation of the Effect of Groove Location and Supply Pressure on the THD Performance of a Steadily Loaded Journal Bearing", *Journal of Tribology*, vol. ۱۲۲, pp.۲۲۷-۲۳۲, January ۲۰۰۰.

۱۷. **Pierre, and M. Fillon**, "Influence of Geometric Parameters and Operating Conditions on the Thermohydrodynamic Behavior of Plain Journal Bearing", *Prose Instn. Mech. Eng. Vol. ۲۱۴ part J: J Engineering Tribology*, pp.۴۴۰-۴۵۷, ۲۰۰۰.

۱۸. **K. Hatakenaka, and M. Tanaka**, "Thermohydrodynamic Performance of Journal Bearings with Partial Reverse Flow and Finger-Type Cavitation", *Prose Instn. Mech. Eng. Vol. ۲۱۶ part J: J Engineering Tribology*, pp.۳۱۵-۳۲۵, ۲۰۰۲.

۱۹. **S. A. Nassab, and M. S. Moayeri**, "Three-Dimensional Thermohydrodynamic Analysis of Axially Grooved Journal Bearings", *Prose Instn. Mech. Eng. Vol. ۲۱۶ part J: J Engineering Tribology*, pp.۳۰-۴۷, ۲۰۰۲.

۲۰. **J. Y. Jang, and M. M. Khonsari**, "Design of Bearing on the Basis of Thermohydrodynamic Analysis", *Prose Instn. Mech. Eng. Vol. ۲۱۸ part J: J Engineering Tribology*, pp.۳۰۰-۳۶۳, ۲۰۰۴.

۲۱. **Gwidon W. Stachowiak, and Andrew W. Batchelor**, "ENGINEERING TRIBOLOGY", Butterworth-Heinemann, (۲۰۰۱), PP.۱۴۷-۱۴۸

۲۲. **A. CAMERON**, "THE PRINCIPLES OF LUBRICATION", *Mechanical Engineering Imtdrial collage*, (۱۹۶۴), PP.۲۹۲-۲۹۳

